Table 2. Peptides

Peptide	Source	Start Position	Amino Acid Sequence	HLA Restriction	Score*
$hTERT_{1088}$	hTERT	1088	TYVPLLGSL	HLA-A24	432
$hTERT_{845}$	hTERT	845	CYGDMENKL	HLA-A24	317
$hTERT_{167}$	hTERT	167	AYQVCGPPL	HLA-A24	300
$hTERT_{461}$	hTERT	461	VYGFVRACL	HLA-A24	280
$hTERT_{324}$	hTERT	324	VYAETKHFL	HLA-A24	240
$hTERT_{1009}$	hTERT	1009	AYRFHACVL	HLA-A24	200
$hTERT_{385}$	hTERT	385	RYWQMRPLF	HLA-A24	200
$hTERT_{637}$	hTERT	637	DYVVGARTF	HLA-A24	150
$hTERT_{622}$	hTERT	622	RFIPKPDGL	HLA-A24	72
$hTERT_{869}$	hTERT	869	DFLLVTPHL	HLA-A24	42
HIV env_{584}	HIV envelope	584	RYLRDQQLL	HLA-A24	720
CMV $pp65_{328}$	CMV pp65	328	QYDPVAALF	HLA-A24	168
HCV $NS3_{1031}$	HCV NS3	1031	AYSQQTRGL	HLA-A24	200
AFP_{137}	AFP	137	PLFQVPEPV	HLA-A2	3

*Estimated half-time of dissociation from the HLA-A24 or -A2 allele (min).

histologically classified as 15 well, 21 moderately, and 1 poorly differentiated HCC. Other patients were diagnosed with HCC based on typical CT findings and an elevation of AFP. The tumors were categorized as "large" (>2 cm) in 44 cases and "small" (≤2 cm) in 28 cases, and as "multiple" (≥2 nodules) in 39 cases and "solitary" (single nodule) in 33 cases. Vascular invasion of the HCC was observed in 15 cases. According to the TNM staging of the Union Internationale Contre Le Cancer (UICC) classification system (6^{th} version),[34] 30, 26, 9, 1, 2, and 4 patients were classified as having stages I, II, IIIA, IIIB, IIIC, and IV disease, respectively.

Selection of Potential HLA-A24–Binding Peptides Within hTERT. To identify potential HLA-A24–binding peptides, the amino acid sequences of hTERT were analyzed using a computer program designed to predict HLA-binding peptides based on the estimation of the half-time dissociation of the HLA–peptide complex. Ten peptides were selected according to the half-time dissociation scores (Table 2). Two of the 10 peptides have been reported to contain HLA-A*2402–restricted epitopes (peptides $hTERT_{461}$ and $hTRERT_{324}$).[35] Next, MHC stabilization assays were performed to test the HLA-A*2402–binding capacity of these peptides using T2-A24 cells. Most peptides increased HLA-A24 expression, indicating that they bound and stabilized the HLA complex on the cell surface (Fig. 1). Peptide CMV$pp65_{328}$, which is identified as a strong binder of the HLA-A*2402 molecule,[25] also increased HLA-A24 expression. Percent MFI increase of the tested peptides except for peptides $hTERT_{1009}$, $hTERT_{385}$, and $hTERT_{622}$ was greater than that of peptide AFP_{137}, which is HLA-A2 restricted.[26]

Immunogenicity of hTERT Peptides in HLA-A*2402/K^b Transgenic Mice. To determine whether these HLA-A24–binding peptides include HLA-A*2402–restricted T cell epitopes, HLA-A*2402/K^b transgenic mice were immunized with hTERT cDNA, and the spleen cell responses were evaluated by interferon gamma (IFN-γ) ELISPOT. Six of 10 hTERT-derived peptides were recognized by the spleen cells of at least one of the primed mice (Fig. 2). Peptides $hTERT_{1009}$, $hTERT_{385}$, $hTERT_{622}$, and $hTERT_{869}$ were not recognized by any mice. These results show that peptides $hTERT_{1088}$, $hTERT_{845}$, $hTERT_{167}$, $hTERT_{461}$, $hTERT_{324}$, and $hTERT_{637}$ may be immunogenic and contain the epitopes restricted by HLA-A*2402.

T Cell Responses to hTERT-Derived Peptides Assessed by IFN-γ ELISPOT Analysis in HCC Patients. To determine whether these HLA-A24–binding peptides could be recognized by the T cells of patients with HCC, PBMC responses were evaluated by IFN-γ ELISPOT. Six of 10 hTERT-derived peptides were recognized by PBMCs of at least one patient, and 29 of 72 patients (40.3%) responded to at least one of the analyzed hTERT-derived peptides. An overview of all responses is shown in Fig. 3A. Single hTERT epitope-specific IFN-γ–producing cells were detected in 6 (8.3%), 6 (8.3%), 9 (12.5%), 5 (6.9%), 9 (12.5%), and 9 (12.5%) of 72 patients in response to the stimulation with peptides $hTERT_{1088}$, $hTERT_{845}$, $hTERT_{167}$, $hTERT_{461}$, $hTERT_{324}$, and $hTERT_{637}$, respectively. Peptides $hTERT_{1009}$, $hTERT_{385}$, $hTERT_{622}$, and $hTERT_{869}$ were not recognized by any patient.

The peptides recognized by PBMCs of the patients with HCC were comparable to those recognized by spleen cells of hTERT cDNA-immunized HLA-A*2402/K^b transgenic mice. These peptides also displayed a relatively high affinity for the HLA-A*2402 molecule compared with the negative control peptide (Fig. 1). The strength of the hTERT-specific T cell responses assessed by the frequencies of IFN-γ–producing cells in the PBMC population is between 10 and 100 specific cells per 3×10^5 PBMCs. Peptide CMV$pp65_{328}$, which includes an

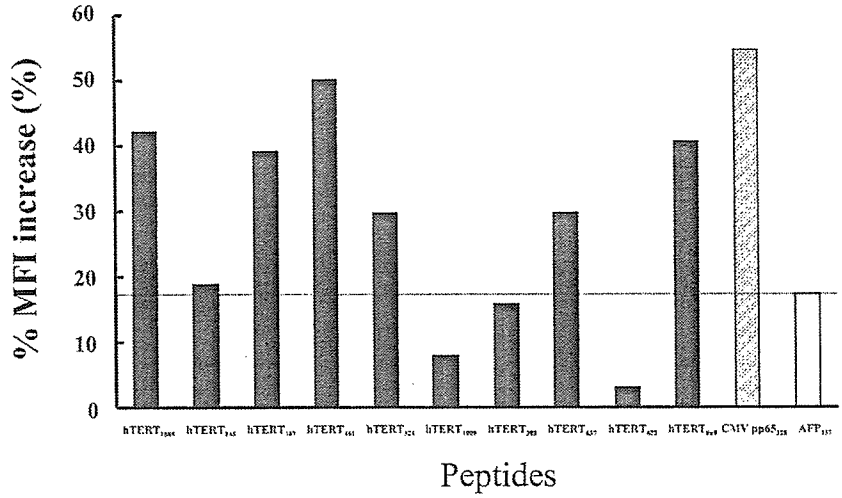

Fig. 1. MHC binding affinity. TAP-deficient T2-A24 cells were cultured for 16 hours at 26°C to enhance the expression of peptide-receptive cell surface molecules. They were incubated with individual peptides at 10 μg/mL at 37°C for 2 hours, washed, and stained with anti-HLA-A24 monoclonal antibody, anti-mouse immunoglobulin-conjugated FITC, and 1 μg propidium iodide per milliliter. The data are expressed as the percent mean fluorescence intensity (MFI) increase for live, propidium iodide-negative cells. Peptide CMVpp65$_{328}$, a previously identified CMV pp65-derived peptide known to be a strong binder to HLA-A24, was used as a positive control. Peptide AFP$_{137}$, a previously identified AFP-derived peptide known to be HLA-A2 restricted, was used as a negative control. The experiment was performed three times, and a representative result is shown. MHC, major histocompatibility complex; HLA, human leukocyte antigen; FITC, fluorescein isothiocyanate; CMV, cytomegalovirus.

epitope derived from the CMV pp65 protein, and HCVNS3$_{1031}$, which includes an epitope derived from the HCV NS3 protein, were also recognized by PBMCs of 31 of 72 (40%) and 12 of 51 (24%) patients with HCC, respectively. Conversely, no patients showed positive T cell responses against peptide HIVenv$_{584}$ derived from the HIV envelope protein, suggesting that these T cell responses were antigen-specific.

In contrast to the results for HCC patients, the ELISPOT assays for the healthy donors did not show more than 10 specific spots for all hTERT-derived peptides (Fig. 3B). The numbers of specific spots (mean ± SD) in the healthy donors were 1.4 ± 1.7, 0.6 ± 0.8, 0.8 ± 1.1, 0.7 ± 1.2, 0.5 ± 0.7, 0.6 ± 1.2, 2.0 ± 2.6, 1.7 ± 2.6, 1.6 ± 3.4, and 1.9 ± 2.9 for hTERT$_{1088}$, hTERT$_{845}$, hTERT$_{167}$, hTERT$_{461}$, hTERT$_{324}$,

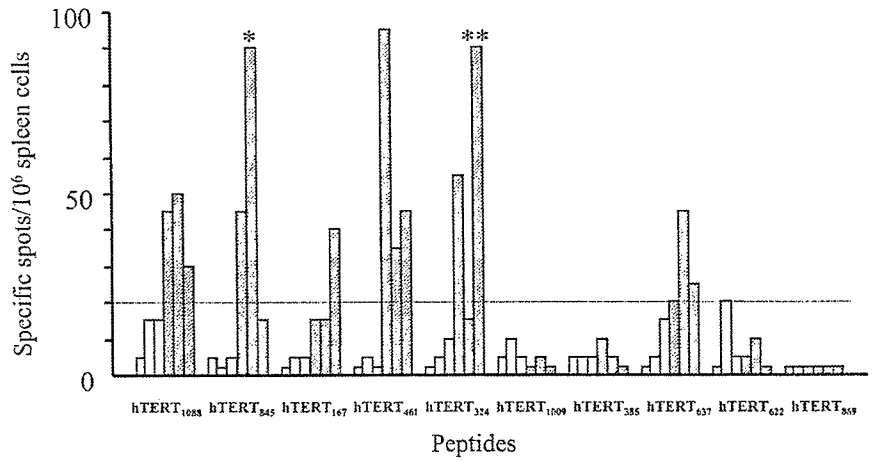

Fig. 2. Direct *ex vivo* analysis (IFN-γ ELISPOT assay) of spleen cell responses to hTERT-derived peptides in hTERT cDNA (hatched bars) or β-gal cDNA (open bars)-immunized HLA-A*2402/K^b transgenic mice. The immunization was performed in three mice for each cDNA. A positive T cell response was defined as more than 20 specific spots/1 × 10^6 spleen cells, which was the maximum response in β-gal cDNA-immunized mice. The peptide sequences are described in Table 2. * denotes 450 specific spots, ** denotes 130 specific spots. IFN-γ, interferon gamma; hTERT, human telomerase reverse transcriptase.

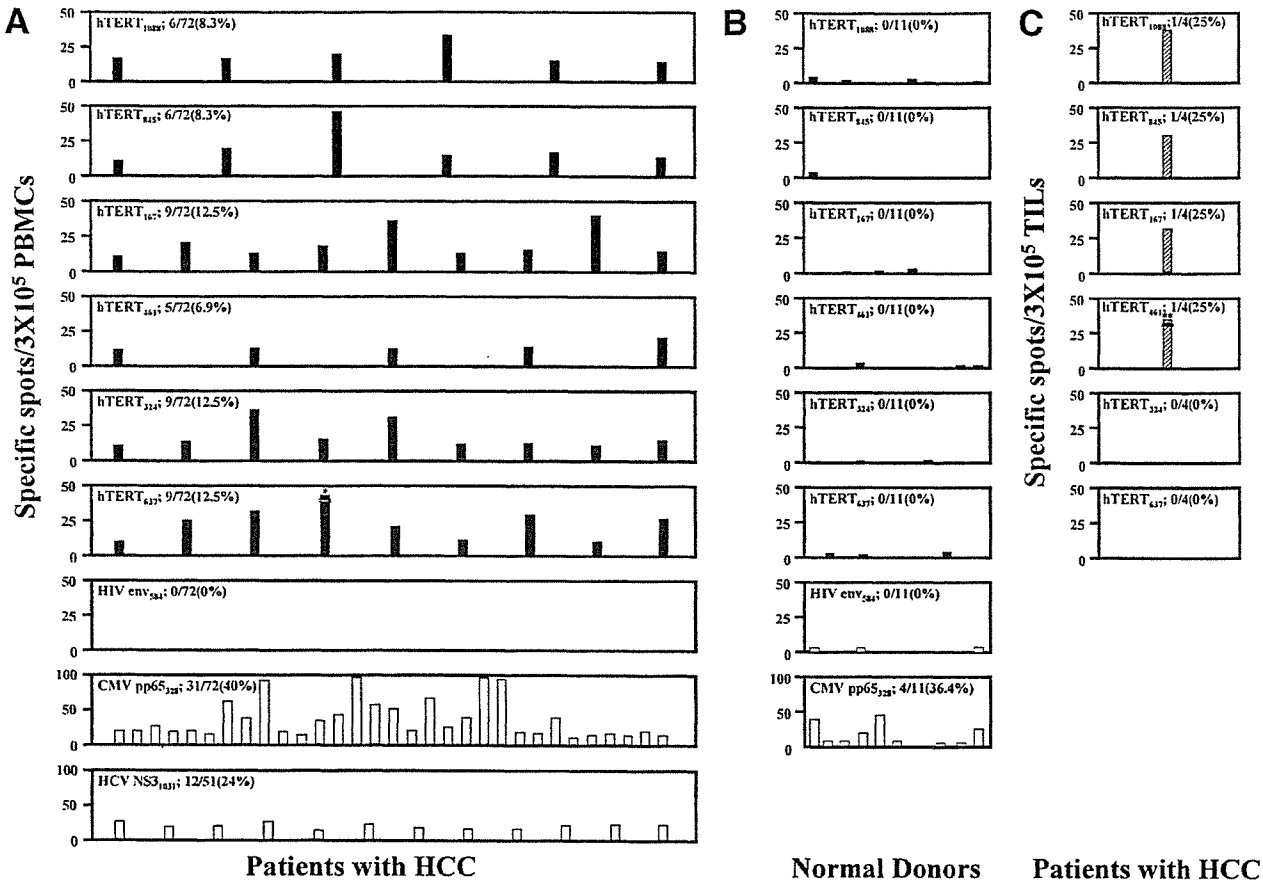

Fig. 3. Direct *ex vivo* analysis (IFN-γ ELISPOT assay) of peripheral blood T cell responses to hTERT-derived peptides (peptides $hTERT_{1088}$, $hTERT_{845}$, $hTERT_{167}$, $hTERT_{461}$, $hTERT_{324}$, and $hTERT_{637}$; solid bars) or control peptides (Peptides $HIVenv_{584}$, $CMVpp65_{328}$ and $HCVNS3_{1031}$; open bars) in HCC patients (A) and normal donors (B). Direct *ex vivo* analysis of tumor-infiltrating lymphocyte responses to hTERT-derived peptides (hatched bars) in HCC patients (C). Only significant IFN-γ responses are included in A and C. Responses were considered positive if more than 10 specific spots were detected and if the number of spots in the presence of antigen was at least twofold greater than that in the absence of antigen. The peptide sequences are described in Table 2. The data for peptides $hTERT_{1009}$, $hTERT_{385}$, $hTERT_{622}$, and $hTERT_{869}$ are excluded because there was no positive T cell response. * denotes 100 specific spots. ** denotes 243 specific spots. IFN-γ, interferon gamma; hTERT, human telomerase reverse transcriptase; HCC, hepatocellular carcinoma.

$hTERT_{1009}$, $hTERT_{385}$, $hTERT_{637}$, $hTERT_{622}$, and $hTERT_{869}$ peptides, respectively. The proportion of normal donors who showed positive T cell responses to CMV protein-derived peptides and the frequencies of the specific T cells were virtually the same as those of the HCC patients (Fig. 3B).

In ELISPOT assay using TILs, IFN-γ–producing T cells responding to peptides $hTERT_{1088}$, $hTERT_{845}$, $hTERT_{167}$, and $hTERT_{461}$ were detected as shown in Fig 3C, suggesting that hTERT-specific TILs were functional.

Cytotoxic Activity Against hTERT-Derived Peptides in HCC Patients. All hTERT-derived peptides were tested for their potential to induce HLA-A24–restricted CTLs from PBMCs of HCC patients with HLA-A24. Each peptide was tested on at least 10 patients. After three rounds of stimulation with the synthetic peptides, responder cells that had been stimulated with peptides $hTERT_{1088}$, $hTERT_{845}$, $hTERT_{167}$, $hTERT_{461}$, $hTERT_{324}$, and $hTERT_{637}$ lysed the peptide-pulsed C1R-A*2402 cells as shown in Fig. 4. Conversely, other peptides failed to induce CTLs specific for the corresponding peptides.

Cytotoxic Activity of hTERT Peptide-Specific CTLs Against Hepatoma Cell Lines. To examine whether hTERT peptide-specific CTLs induced from PBMCs of HCC patients lyse hepatoma cell lines that express hTERT, we first checked the telomerase activity in three hepatoma cells. TRAP assays showed that the three hepatoma cells expressed hTERT; however, the expression in HuH6 cells was lower than that in HepG2 or HuH7 cells (Fig. 5A). The results were confirmed in the TRAP ELISA, which is a quantitative measurement of telomerase activity. The expression levels of hTERT in HepG2 and HuH7 cells were more than twofold higher than the level in HuH6 cells (Fig. 5B).

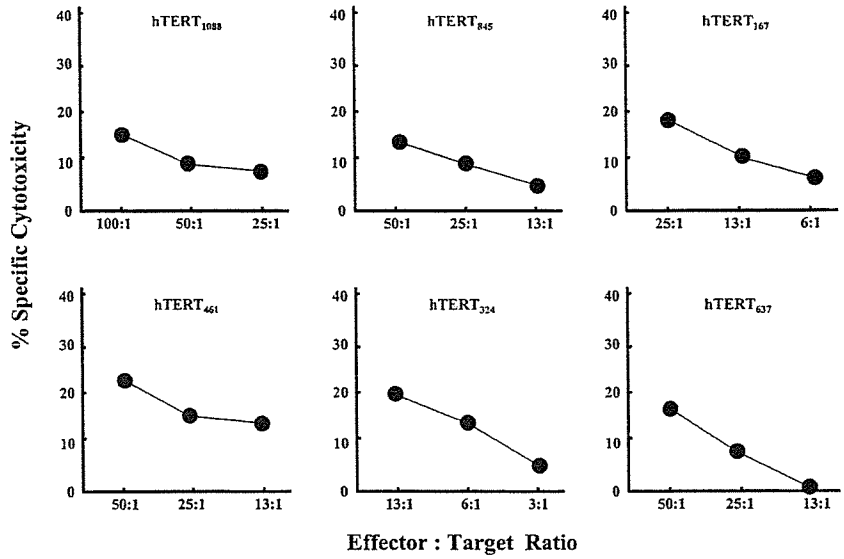

Fig. 4. Cytotoxicity of hTERT-specific T-cell lines derived with peptide in patients with HCC. The cytotoxicity of the T-cell lines was determined by a standard 6-hour cytotoxicity assay at various effector to target (E/T) ratios against C1R-A*2402 cells pulsed with one of the hTERT-derived peptides listed in Table 2. The data are indicated as the percent specific cytotoxicity, which is calculated as follows: (cytotoxicity in the presence of specific peptide) − (cytotoxicity in the absence of peptide). hTERT, human telomerase reverse transcriptase; HCC, hepatocellular carcinoma.

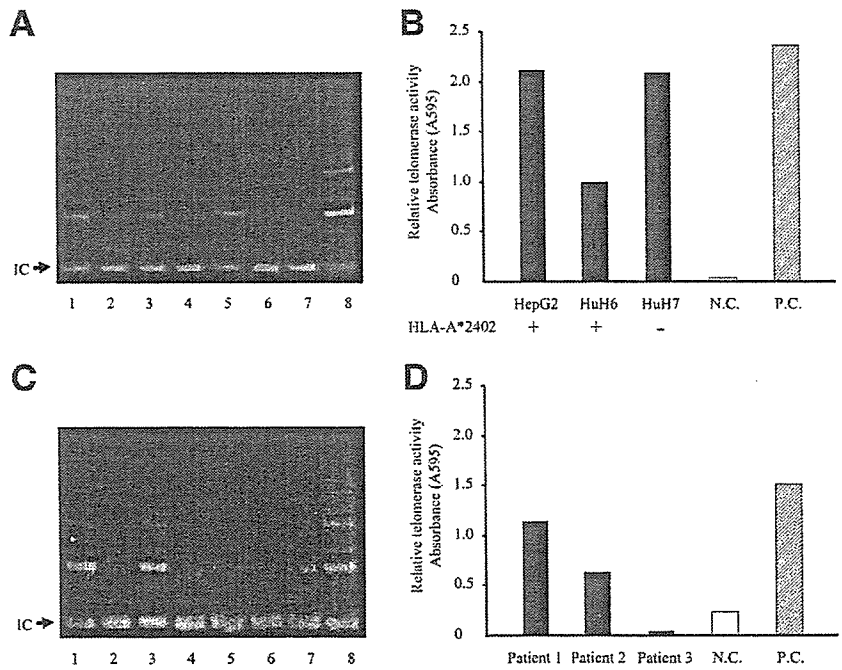

Fig. 5. Telomerase activity in hepatoma cell lines (A, B) and tumors resected by surgical treatment (C, D). A TRAP assay was carried out with 0.01 μg and 0.1 μg cell extract from hepatoma cell lines and tumors, respectively. The products of the PCR were fractionated by electrophoresis on a 10% polyacrylamide gel and then visualized by staining with SYBR-Green I. The TRAP internal control (IC) is shown for each extract. A: Lane 1; HepG2, Lane 2; HepG2 with heat, Lane 3; HuH 6, Lane 4; HuH 6 with heat, Lane 5; HuH 7, Lane 6; HuH 7 with heat, Lane 7; negative control, Lane 8; positive control. B: Lanes 1, 3, and 5, HCCs from three different patients; Lanes 2, 4, and 6, HCCs from three different patients with heat; Lane 7, negative control; Lane 8, positive control. Relative telomerase activity was measured with a TRAPEZE ELISA telomerase detection kit (TRAP ELISA) in hepatoma cell lines (C) and tumors resected by surgical treatment (D). Molecular typing of the HLA-A allele for hepatoma cell lines was performed with genomic DNA using standard site-specific oligonucleotide PCR. NC, negative control; PC, positive control; TRAP, telomerase repeat amplification protocol; PCR, polymerase chain reaction; HCC, hepatocellular carcinoma.

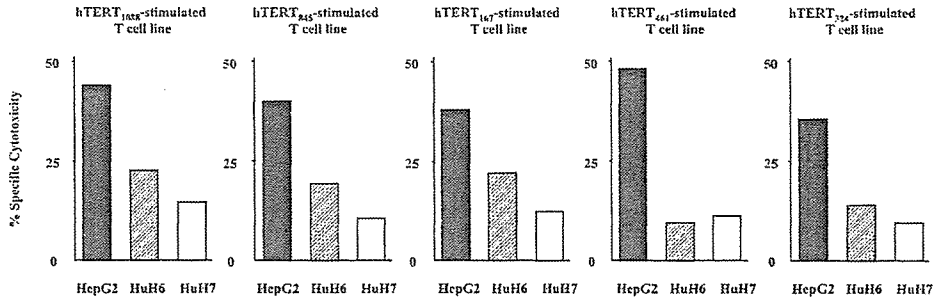

Fig. 6. Cytotoxicity of hTERT-specific T-cell lines derived with peptide against hepatoma cell lines. HepG2 (solid bar) highly expresses hTERT and has HLA-A*2402. HuH 6 (hatched bar) shows low expression of hTERT and has HLA-A*2402. HuH 7 (open bar) shows hTERT expression of the same level as HepG2 but does not have HLA-A*2402. The cytotoxicity was determined by a standard 6-hour cytotoxic assay (E/T ratio of 50:1). hTERT, human telomerase reverse transcriptase.

We next examined the cytotoxicity of hTERT peptide–specific CTLs against these hepatoma cell lines. As shown in Fig. 6, peptides $hTERT_{1088}$, $hTERT_{845}$, $hTERT_{167}$, $hTERT_{461}$, and $hTERT_{324}$-specific CTLs showed cytotoxicity against HepG2 cells, which highly express hTERT and has the HLA-A*2402 molecule. In contrast, the CTLs did not show cytotoxicity against HuH7 cells, which express hTERT at the same level as HepG2 cells but do not have HLA-A*2402. In addition, the cytotoxicity of hTERT-specific CTLs induced with peptides $hTERT_{1088}$, $hTERT_{845}$, $hTERT_{167}$, and $hTERT_{324}$ against HuH6 cells, which express HLA-A*2402 and a low level of hTERT, was weak compared with the cytotoxicity against HepG2 cells. The difference was even more marked in the cytotoxicity of CTLs induced with peptide $hTERT_{461}$, and the CTLs were not cytotoxic to HuH6 cells.

Telomerase activity was also detected in the tumor of 3 of 10 patients with HCC (Fig. 5C and D). All of the three patients showed hTERT-specific T cell responses in ELISPOT assay.

Detection of $hTERT_{461}$ Tetramer$^+$ and CD8$^+$ T Lymphocytes in PBMCs and TILs. To analyze the character of hTERT specific T cells in patients with HCC more precisely, we examined the frequencies of $hTERT_{461}$ tetramer$^+$ cells in PBMCs and TILs, and compared them with the results of ELISPOT assay. PBMCs and TILs were stained with CD4-FITC, CD14-FITC, CD19-FITC, CD8-PerCP, and tetramer-PE as described in Patients and Methods. At least 1×10^5 cells in the $CD8^+CD4^-CD14^-CD19^-$ gate were then analyzed for tetramer staining as shown in Fig. 7A.

As indicated in Fig. 7B, the frequencies of $CD8^+$ $CD4^-CD14^-CD19^-hTERT_{461}$ tetramer$^+$ cells in peripheral blood were 0.03% to 0.71% of $CD8^+$ T cells (patients 1-15). The frequencies in the patients with positive responses for ELISPOT assay were 0.06% to 0.71%. Interestingly, 7 of 10 patients without positive responses for ELISPOT assay showed 0.07% to 0.26% $CD8^+$ $CD4^-CD14^-CD19^-hTERT_{461}$tetramer$^+$ cells. These results suggest that dysfunctional hTERT-specific T cells exist in patients with HCC. Conversely, the frequency of $CD8^+CD4^-CD14^-CD19^-hTERT_{461}$ tetramer$^+$ cells in TILs was quite high (2.73%), and they were functional (patient 16).

hTERT-Specific T Cell Responses and Clinical Features of HCC Patients. To evaluate the status of hTERT-specific T cell responses in patients with HCC,

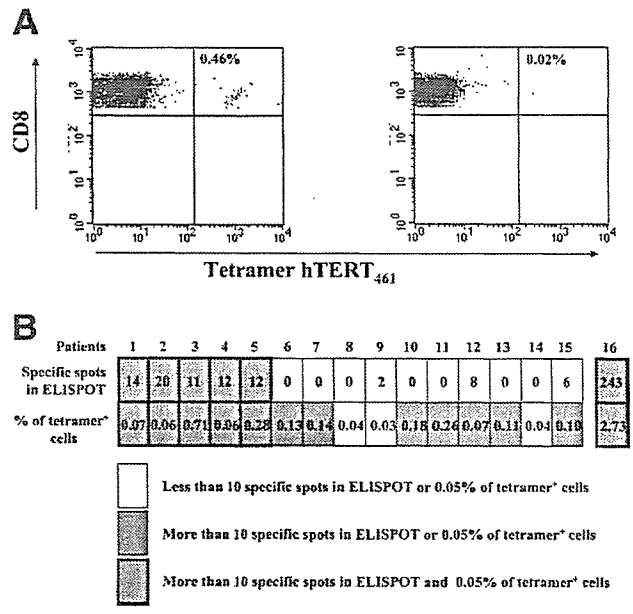

Fig. 7. Detection of hTERT-specific, HLA-A*2402-tetramer$^+$, $CD8^+CD4^-CD14^-$ $CD19^-$ T lymphocytes in the peripheral blood and tumor. PBMCs isolated from representative patients with HCC (A) were stained with tetrameric complexes and antibodies and analyzed on a FACSCalibur™ flow cytometer. Analysis of the association between the frequency of tetramer$^+$ cells and IFN-γ-producing cells detected in ELISPOT assay (B). Tetramer staining and ELISPOT assay were performed in 16 patients using PBMCs (patients 1-15) and TILs (patient 16). hTERT, human telomerase reverse transcriptase; PBMC, peripheral blood mononuclear cell; HCC, hepatocellular carcinoma; IFN-γ, interferon gamma; TIL, tumor-infiltrating lymphocyte.

Table 3. Univariate Analysis of the Effect of Variables on the T Cell Response Against hTERT

	Patients With Positive T Cell Response	Patients Without Positive T Cell Response	P
No. of patients	29	43	
Age (years)*	67.7 ± 9.7	66.7 ± 8.1	NS
Sex (M/F)	21/8	27/16	NS
AFP level (≦20/> 20)	13/16	14/29	NS
Diff. degree of HCC (well/moderate or poor/ND[c])	9/6/14	6/16/21	NS
Tumor multiplicity (multiple/solitary)	17/12	22/21	NS
Vascular invasion (+/−)	7/22	8/35	NS
TNM factor			
(T1/T2-4)	11/18	19/24	NS
(N0/N1)	28/1	43/0	NS
(M0/M1)	29/0	39/4	NS
TNM stage (I/II-IV)	11/18	19/24	NS
Histology of non-tumor liver (LC/Chronic hepatitis)	25/4	39/4	NS
Liver function (Child A/B/C)	13/14/2	30/11/2	NS
Etiology (HCV/HBV/Others)	22/3/4	37/6/0	NS

Abbreviations: NS; there was no statistical significance; ND, not determined.
*Data are expressed as mean ± SD.

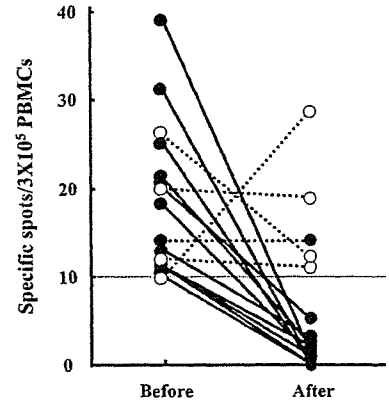

Fig. 8. Kinetics of hTERT-specific T cell responses before and after curative treatments. PBMCs were obtained before and 6 months after treatments and analyzed. Open circles show the patients without tumor recurrence within 1 year after treatment. Closed circles show the patients with tumor recurrence within 1 year after treatment. Solid and dotted lines show the patients without and with more than 10 specific spots for hTERT-derived peptides in ELISPOT assay after treatment, respectively. hTERT, human telomerase reverse transcriptase; PBMC, peripheral blood mononuclear cell.

we analyzed the relationship between the frequencies of peptides $hTERT_{1088}$, $hTERT_{845}$, $hTERT_{167}$, $hTERT_{461}$, $hTERT_{324}$, and $hTERT_{637}$-specific T cells detected by IFN-γ ELISPOT assay and the clinical features of patients. Table 3 shows clinical features of HCC patients who showed positive and negative T cell responses to hTERT-derived epitopes.

The clinical features of both groups were not statistically different in terms of age, sex, serum AFP levels, differentiation of HCC, tumor multiplicity, vascular invasion, TNM factors and stages, histology of the non-tumor liver, liver function, and the type of viral infection (Table 3).

Next, we examined the kinetics of hTERT-specific T cells in 16 patients who had positive T cell responses and received curative treatments by surgical resection or radiofrequent ablation, and analyzed the association between the kinetics and clinical responses. The frequencies of hTERT-specific T cells detected in ELISPOT assay decreased in most of the patients 6 months after curative treatments (Fig. 8). Only 5 of 16 patients showed positive T cell responses after treatments. Four patients whose hTERT-specific T cells were maintained had no recurrence of HCC. In contrast, 11 patients whose number of hTERT-specific T cells decreased showed HCC recurrence within 1 year after curative treatments.

Discussion

In the current study, we first attempted to identify hTERT epitopes restricted by HLA-A24, which is present in 60% of Japanese, 20% of whites, and 12% of Africans,[36,37] using a combined computer-based and immunological approach. Analysis of amino acid sequences of hTERT by computer showed a number of potential HLA-A24–binding peptides, and 2 of the 10 hTERT-derived peptides (Peptides $hTERT_{461}$ and $hTERT_{324}$) have been identified to contain HLA-A24–restricted CTL epitopes. Including these two peptides, six hTERT-derived peptides (peptides $hTERT_{1088}$, $hTERT_{845}$, $hTERT_{167}$, $hTERT_{461}$, $hTERT_{324}$, and $hTERT_{637}$) that showed high affinity for HLA-A*2402 induced production of IFN-γ in spleen cells and PBMCs, in hTERT cDNA-immunized HLA-A*2402/K^b transgenic mice and HCC patients, respectively. In addition, T cell lines stimulated with the peptide showed cytotoxicity against hepatoma cell lines that express HLA-A*2402 and hTERT. Taken together with the results of peptide binding, ELISPOT, and CTL assay, we concluded peptides $hTERT_{1088}$, $hTERT_{845}$, $hTERT_{167}$, $hTERT_{461}$, $hTERT_{324}$, and $hTERT_{637}$ contained HLA-A24 restricted, hTERT-specific CTL epitopes.

Interestingly, the cytotoxicity of hTERT-specific CTLs induced with peptides $hTERT_{1088}$, $hTERT_{845}$, $hTERT_{167}$, and $hTERT_{324}$ in HuH6 cells, which showed low levels of hTERT, was weak compared with the cytotoxicity in HepG2 cells with high levels of hTERT. The difference was even more marked in the cytotoxicity of CTLs induced with peptide $hTERT_{461}$, and the CTLs were not cytotoxic to HuH6. In accordance with our results, it was reported that the susceptibility of tumor cells to hTERT-specific CTLs decreased after IFN-γ

treatment because of attenuation of hTERT expression.[38] In addition, all of the patients who had telomerase activity in the tumor showed hTERT-specific T cell responses in ELISPOT assay. These results suggest that the strength of hTERT-specific cytotoxicity against hepatoma cells depends on the expression levels of the protein.

In the analysis of PBMCs in patients with HCC using $hTERT_{461}$ tetramer, the frequencies of $hTERT_{461}$ tetramer$^+$ cells in PBMCs were similar to those of other tumor specific antigen-derived epitopes.[39] Furthermore, the existence of dysfunctional hTERT-specific T cells was accordant with previous reports of other tumor antigens.[39] Conversely, the frequency of $hTERT_{461}$ tetramer$^+$ cells in tumors was quite high, and they produced IFN-γ. IFN-γ–producing T cells responding to other peptides $hTERT_{1088}$, $hTERT_{845}$, and $hTERT_{167}$ were also detected in tumors. These results suggest that hTERT is an attractive target for immunotherapy of HCC.

In the second part of the current study, to study the status of the host immunological response to hTERT in HCC patients, we examined the frequency of hTERT-specific T cells in the peripheral blood by ELISPOT assay with the six epitopes and analyzed the relationship between the frequency and the clinical features of the patients. ELISPOT assay showed that the frequency of reactive T cells to a single hTERT epitope was 10 to 100 per 3×10^5 PBMCs. In previous reports regarding the frequency of T cells specific for a single hTERT epitope in patients with colon or breast cancer, the number was found to be 1 to 22 per 2×10^5 PBMCs or 1 to 33 per 2×10^5 PBMCs, respectively.[18,19] In addition, single hTERT epitope–specific IFN-γ–producing cells were detected in 6.9% to 12.5% of the patients for peptides $hTERT_{1088}$, $hTERT_{845}$, $hTERT_{167}$, $hTERT_{461}$, $hTERT_{324}$, and $hTERT_{637}$. These rates are quite similar to those in previous reports.[18,19] Comparing the current results with those reports, we believe that hTERT-specific CTL responses in HCC patients are as strong as those of other cancer patients and that the newly identified hTERT epitopes are immunogenic.

From the analysis of hTERT-specific immune responses in HCC patients, we obtained evidence that clinical features, including age, sex, serum AFP levels, differentiation of HCC, tumor multiplicity, vascular invasion, TNM factors and stages, histology of the nontumor liver, liver function, and the type of viral infection, were not associated with the frequency of hTERT-specific CTLs in HCC patients (Table 3). These results suggest that hTERT-specific CTLs could be generated independently of hepatitis viral infection or serum AFP levels, which suppress the host immune response through inhibition of dendritic cells[40-42] or T cell proliferation.[43] In addition, comparing with AFP- or other tumor antigen–specific immune responses,[31,44] hTERT-specific immune responses exist and can be induced in the patients with HCC even at early stages. These results suggest the advantage of hTERT as a target for immunotherapies because the induction of tumor-specific immune responses at early stages of the tumor should be more effective for tumor growth suppression.

In the analysis of the association between kinetics of hTERT-specific T cells and clinical responses, recurrent rate of HCC was higher in the patients without maintenance of hTERT-specific T cells than in those with. This result suggests that maintenance of hTERT-specific T cells may be important to protect tumor recurrence after treatments, although there was no statistically significant difference between the two groups because of the small number of patients.

In conclusion, we identified and characterized HLA-A*2402–restricted T cell epitopes derived from hTERT. The identified epitope-specific T cells can be detected and induced by stimulating PBMCs with these peptides in HCC patients. hTERT-specific CTLs were observed even in the patients with early stages of HCC and killed hepatoma cell lines that expressed hTERT dependent on the expression level. The frequency of hTERT/tetramer$^+$CD8$^+$ T cells in the tumor tissue of patients with HCC was quite high, and they were functional. These results suggest that hTERT is an important target of T-cell–based immunotherapy for HCC and that the identified epitopes could be valuable both for therapy and for analyzing the host immune responses.

Acknowledgment: The authors thank Maki Kawamura, Sanae Funaoka, and Chiharu Minami for their invaluable help with sample collection, and all patients who donated blood samples for this study.

References

1. Parkin DM, Bray F, Ferlay J, Pisani P. Estimating the world cancer burden: Globocan 2000. Int J Cancer 2001;94:153-156.
2. El-Serag HB, Mason AC. Rising incidence of hepatocellular carcinoma in the United States. N Engl J Med 1999;340:745-750.
3. Deuffic S, Poynard T, Buffat L, Valleron AJ. Trends in primary liver cancer. Lancet 1998;351:214-215.
4. Curley SA, Izzo F, Ellis LM, Nicolas Vauthey J, Vallone P. Radiofrequency ablation of hepatocellular cancer in 110 patients with cirrhosis. Ann Surg 2000;232:381-391.
5. Urabe T, Kaneko S, Matsushita E, Unoura M, Kobayashi K. Clinical pilot study of intrahepatic arterial chemotherapy with methotrexate, 5-fluorouracil, cisplatin and subcutaneous interferon-alpha-2b for patients with locally advanced hepatocellular carcinoma. Oncology 1998;55:39-47.
6. Mazzaferro V, Regalia E, Doci R, Andreola S, Pulvirenti A, Bozzetti F, et al. Liver transplantation for the treatment of small hepatocellular carcinomas in patients with cirrhosis. N Engl J Med 1996;334:693-699.
7. Meyerson M, Counter CM, Eaton EN, Ellisen LW, Steiner P, Caddle SD, et al. hEST2, the putative human telomerase catalytic subunit gene, is up-regulated in tumor cells and during immortalization. Cell 1997;90:785-795.

8. Nakamura TM, Morin GB, Chapman KB, Weinrich SL, Andrews WH, Lingner J, et al. Telomerase catalytic subunit homologs from fission yeast and human. Science 1997;277:955-959.
9. Nakayama J, Tahara H, Tahara E, Saito M, Ito K, Nakamura H, et al. Telomerase activation by hTRT in human normal fibroblasts and hepatocellular carcinomas. Nat Genet 1998;18:65-68.
10. Harrington L, Zhou W, McPhail T, Oulton R, Yeung DS, Mar V, et al. Human telomerase contains evolutionarily conserved catalytic and structural subunits. Genes Dev 1997;11:3109-3115.
11. Vonderheide RH, Hahn WC, Schultze JL, Nadler LM. The telomerase catalytic subunit is a widely expressed tumor-associated antigen recognized by cytotoxic T lymphocytes. Immunity 1999;10:673-679.
12. Vonderheide RH, Anderson KS, Hahn WC, Butler MO, Schultze JL, Nadler LM. Characterization of HLA-A3-restricted cytotoxic T lymphocytes reactive against the widely expressed tumor antigen telomerase. Clin Cancer Res 2001;7:3343-3348.
13. Scardino A, Gross DA, Alves P, Schultze JL, Graff-Dubois S, Faure O, et al. HER-2/neu and hTERT cryptic epitopes as novel targets for broad spectrum tumor immunotherapy. J Immunol 2002;168:5900-5906.
14. Saeboe-Larssen S, Fossberg E, Gaudernack G. mRNA-based electrotransfection of human dendritic cells and induction of cytotoxic T lymphocyte responses against the telomerase catalytic subunit (hTERT). J Immunol Methods 2002;259:191-203.
15. Frolkis M, Fischer MB, Wang Z, Lebkowski JS, Chiu CP, Majumdar AS. Dendritic cells reconstituted with human telomerase gene induce potent cytotoxic T-cell response against different types of tumors. Cancer Gene Ther 2003;10:239-249.
16. Parkhurst MR, Riley JP, Igarashi T, Li Y, Robbins PF, Rosenberg SA. Immunization of patients with the hTERT:540-548 peptide induces peptide-reactive T lymphocytes that do not recognize tumors endogenously expressing telomerase. Clin Cancer Res 2004;10:4688-4698.
17. Verra NC, Jorritsma A, Weijer K, Ruizendaal JJ, Voordouw A, Weder P, et al. Human telomerase reverse transcriptase-transduced human cytotoxic T cells suppress the growth of human melanoma in immunodeficient mice. Cancer Res 2004;64:2153-2161.
18. Amarnath SM, Dyer CE, Ramesh A, Iwuagwu O, Drew PJ, Greenman J. In vitro quantification of the cytotoxic T lymphocyte response against human telomerase reverse transcriptase in breast cancer. Int J Oncol 2004; 25:211-217.
19. Titu LV, Loveday RL, Madden LA, Cawkwell L, Monson JR, Greenman J. Cytotoxic T-cell immunity against telomerase reverse transcriptase in colorectal cancer patients. Oncol Rep 2004;12:871-876.
20. Schreurs MW, Kueter EW, Scholten KB, Kramer D, Meijer CJ, Hooijberg E. Identification of a potential human telomerase reverse transcriptase-derived, HLA-A1-restricted cytotoxic T-lymphocyte epitope. Cancer Immunol Immunother 2005;54:703-712.
21. Araki T, Itai Y, Furui S, Tasaka A. Dynamic CT densitometry of hepatic tumors. AJR Am J Roentgenol 1980;135:1037-1043.
22. Japan. LCSGo. Classification of Primary Liver Cancer. English ed 2. Tokyo:Kanehara & Co.,Ltd. 1997.
23. Desmet VJ, Gerber M, Hoofnagle JH, Manns M, Scheuer PJ. Classification of chronic hepatitis: diagnosis, grading and staging. HEPATOLOGY 1994;19:1513-1520.
24. Ikeda-Moore Y, Tomiyama H, Miwa K, Oka S, Iwamoto A, Kaneko Y, et al. Identification and characterization of multiple HLA-A24-restricted HIV-1 CTL epitopes: strong epitopes are derived from V regions of HIV-1. J Immunol 1997;159:6242-6252.
25. Kuzushima K, Hayashi N, Kimura H, Tsurumi T. Efficient identification of HLA-A*2402-restricted cytomegalovirus-specific CD8(+) T-cell epitopes by a computer algorithm and an enzyme-linked immunospot assay. Blood 2001;98:1872-1881.
26. Butterfield LH, Meng WS, Koh A, Vollmer CM, Ribas A, Dissette VB, et al. T cell responses to HLA-A*0201-restricted peptides derived from human alpha fetoprotein. J Immunol 2001;166:5300-5308.
27. Oiso M, Eura M, Katsura F, Takiguchi M, Sobao Y, Masuyama K, et al. A newly identified MAGE-3-derived epitope recognized by HLA-A24-restricted cytotoxic T lymphocytes. Int J Cancer 1999;81:387-394.
28. Arai K, Masutomi K, Khurts S, Kaneko S, Kobayashi K, Murakami S. Two independent regions of human telomerase reverse transcriptase are important for its oligomerization and telomerase activity. J Biol Chem 2002;277: 8538-8544.
29. Gotoh M, Takasu H, Harada K, Yamaoka T. Development of HLA-A2402/K(b) transgenic mice. Int J Cancer 2002;100:565-570.
30. Mizukoshi E, Nascimbeni M, Blaustein JB, Mihalik K, Rice CM, Liang TJ, et al. Molecular and immunological significance of chimpanzee major histocompatibility complex haplotypes for hepatitis C virus immune response and vaccination studies. J Virol 2002;76:6093-6103.
31. Mizukoshi E, Nakamoto Y, Tsuji H, Yamashita T, Kaneko S. Identification of alpha-fetoprotein-derived peptides recognized by cytotoxic T lymphocytes in HLA-A24+ patients with hepatocellular carcinoma. Int J Cancer 2006;118:1194-204.
32. Wedemeyer H, Mizukoshi E, Davis AR, Bennink JR, Rehermann B. Cross-reactivity between hepatitis C virus and Influenza A virus determinant-specific cytotoxic T cells. J Virol 2001;75:11392-11400.
33. Nakamoto Y, Kaneko S, Takizawa H, Kikumoto Y, Takano M, Himeda Y, et al. Analysis of the CD8-positive T cell response in Japanese patients with chronic hepatitis C using HLA-A*2402 peptide tetramers. J Med Virol 2003;70:51-61.
34. Sobin LH WC. TNM Classification of Malignant Tumors, 6th ed. New York: Wiley-Liss 2002:81.
35. Arai J, Yasukawa M, Ohminami H, Kakimoto M, Hasegawa A, Fujita S. Identification of human telomerase reverse transcriptase-derived peptides that induce HLA-A24-restricted antileukemia cytotoxic T lymphocytes. Blood 2001;97:2903-2907.
36. Imanishi T, Akaza, T, Kimura A, Tokunaga K, Gojobori T. Allele and Haplotype Frequencies for HLA and Complement Loci in Various Ethnic Groups. Oxford Scientific Publications, Oxford 1992:1065-1220.
37. Tokunaga K, Ishikawa Y, Ogawa A, Wang H, Mitsunaga S, Moriyama S, et al. Sequence-based association analysis of HLA class I and II alleles in Japanese supports conservation of common haplotypes. Immunogenetics 1997;46:199-205.
38. Tajima K, Ito Y, Demachi A, Nishida K, Akatsuka Y, Tsujimura K, et al. Interferon-gamma differentially regulates susceptibility of lung cancer cells to telomerase-specific cytotoxic T lymphocytes. Int J Cancer 2004;110: 403-412.
39. Shang XY, Chen HS, Zhang HG, Pang XW, Qiao H, Peng JR, et al. The spontaneous CD8+ T-cell response to HLA-A2-restricted NY-ESO-1b peptide in hepatocellular carcinoma patients. Clin Cancer Res 2004;10: 6946-6955.
40. Kanto T, Hayashi N, Takehara T, Tatsumi T, Kuzushita N, Ito A, et al. Impaired allostimulatory capacity of peripheral blood dendritic cells recovered from hepatitis C virus-infected individuals. J Immunol 1999;162: 5584-5591.
41. Auffermann-Gretzinger S, Keeffe EB, Levy S. Impaired dendritic cell maturation in patients with chronic, but not resolved, hepatitis C virus infection. Blood 2001;97:3171-3176.
42. Beckebaum S, Cicinnati VR, Zhang X, Ferencik S, Frilling A, Grosse-Wilde H, et al. Hepatitis B virus-induced defect of monocyte-derived dendritic cells leads to impaired T helper type 1 response in vitro: mechanisms for viral immune escape. Immunology 2003;109:487-495.
43. Peck AB, Murgita RA, Wigzell H. Cellular and genetic restrictions in the immunoregulatory activity of alpha-fetoprotein. II. Alpha-fetoprotein-induced suppression of cytotoxic T lymphocyte development. J Exp Med 1978;148:360-372.
44. Nagorsen D, Keilholz U, Rivoltini L, Schmittel A, Letsch A, Asemissen AM, et al. Natural T-cell response against MHC class I epitopes of epithelial cell adhesion molecule, her-2/neu, and carcinoembryonic antigen in patients with colorectal cancer. Cancer Res 2000;60:4850-4854.

Different Signaling Pathways in the Livers of Patients With Chronic Hepatitis B or Chronic Hepatitis C

Masao Honda, Taro Yamashita, Teruyuki Ueda, Hajime Takatori, Ryuhei Nishino, and Shuichi Kaneko

The clinical manifestations of chronic hepatitis B (CH-B) and chronic hepatitis C (CH-C) are different. We previously reported differences in the gene expression profiles of liver tissue infected with CH-B or CH-C; however, the signaling pathways underlying each condition have yet to be clarified. Using a newly constructed cDNA microarray consisting of 9614 clones selected from 256,550 tags of hepatic serial analysis of gene expression (SAGE) libraries, we compared the gene expression profiles of liver tissue from 24 CH-B patients with those of 23 CH-C patients. Laser capture microdissection was used to isolate hepatocytes from liver lobules and infiltrating lymphoid cells from the portal area, from 16 patients, for gene expression analysis. Furthermore, the comprehensive gene network was analyzed using SAGE libraries of CH-B and CH-C. Supervised and nonsupervised learning methods revealed that gene expression was correlated more with the infecting virus than any other clinical parameters such as histological stage and disease activity. Pro-apoptotic and DNA repair responses were predominant in CH-B with p53 and 14-3-3 interacting genes having an important role. In contrast, inflammatory and anti-apoptotic phenotypes were predominant in CH-C. These differences would evoke different oncogenic factors in CH-B and CH-C. In conclusion, we describe the different signaling pathways induced in the livers of patients with CH-B or CH-C. The results might be useful in guiding therapeutic strategies to prevent the development of hepatocellular carcinoma in cases of CH-B and CH-C. *Supplementary material for this article can be found on the HEPATOLOGY website (http://interscience.wiley.com/jpages/0270-9139/suppmat/index.html).* (HEPATOLOGY 2006;44:1122-1138.)

The human liver infected with hepatitis B virus (HBV) and hepatitis C virus (HCV) develops chronic hepatitis, cirrhosis, and in some instances, hepatocellular carcinoma (HCC).[1-3] The virological features of these 2 viruses are completely different. HBV is a DNA virus that integrates into the host genome.[4,5] HBV proteins, which have been reported to have transcriptional transactivator activity, may be related to the occurrence of HCC.[6-9] By contrast, HCV is a positive stranded RNA virus that replicates in the cytoplasm.[2] There are some reports that HCV proteins localize to the nucleus or interact with nuclear proteins.[10,11] Nevertheless, both viruses infect the liver and cause chronic hepatitis, which is not distinguishable by histological examination or clinical manifestations.[12] In chronic viral hepatitis, increased numbers of immunoregulatory cells infiltrate the liver, but the functional relevance of these cells to the pathogenesis of chronic hepatitis is not known.

We previously reported that the gene expression profiles in the livers of patients with chronic hepatitis B (CH-B) or chronic hepatitis C (CH-C) are different, and revealed some characteristic features of each disease.[13] However, the independent expression profiles of infiltrated lymphocytes and hepatocytes have yet to be clarified, as do the detailed signaling pathways underlying these 2 conditions.

In this study, we investigated the signaling pathways underlying CH-B and CH-C using cDNA microarray and serial analysis of gene expression (SAGE) techniques. Using laser capture microdissection (LCM), we selectively isolated hepatocytes from liver lobules and infiltrat-

Abbreviations: CH-B, chronic hepatitis B; CH-C, chronic hepatitis C; SAGE, serial analysis of gene expression; HBV, hepatitis B virus; HCV, hepatitis C virus; HCC, hepatocellular carcinoma; GO, gene ontology; LCM, laser capture microdissection; ALT, alanine aminotransferase; aRNA, antisense RNA; CTL, cytotoxic lymphocyte; Cy, cyanine; EGFR, epidermal growth factor receptor; cDNA, complementary DNA; IFN, interferon; NF-κB, nuclear factor-κB; NK cells, natural killer cells.

From the Department of Gastroenterology, Kanazawa University Graduate School of Medicine, Kanazawa, Japan.

Received April 29, 2006; accepted August 8, 2006.

Address reprint requests to: Shuichi Kaneko, M.D., Ph.D., Department of Gastroenterology, Graduate School of Medicine, Kanazawa University, Takara-Machi 13-1, Kanazawa, 920-8641, Japan. E-mail: skaneko@medf.m.kanazawa-u.ac.jp; fax: (81) 76-234-4250.

Published online in Wiley InterScience (www.interscience.wiley.com).

DOI 10.1002/hep.21383

Potential conflict of interest: Nothing to report.

ing lymphoid cells from the portal area, from biopsy specimens, and analyzed their gene expression profiles.

Patients and Methods

Patients. The subjects were 27 patients with CH-B and 26 with CH-C at the Graduate School of Medicine, Kanazawa University Hospital, Japan, between 1999 and 2003 (Table 1). Informed consent was obtained from all patients and ethics approval for the study was obtained from the ethics committee for human genome/gene analysis research at Kanazawa University Graduate School of Medicine. Liver biopsy samples were taken from 24 CH-B patients and 23 CH-C patients, and were divided into 3 portions: one was immersed in formalin for histological assessment, another was immediately frozen in liquid nitrogen for further RNA isolation, and the final portion was frozen in OCT compound for LCM analysis and stored at −80°C until use. Tissue samples from the remaining 6 patients with HCC were surgically obtained from the noncancerous parts of the liver and immediately frozen in liquid nitrogen for SAGE analysis. For normal liver, surgically obtained tissue samples of 6 patients who showed no clinical signs of hepatitis were used, as described.[13]

The grading and staging of chronic hepatitis were histologically assessed according to the method described by Desmet et al.[14] (Table 1). There were no significant differences in the degree of histological activity or staging, nor in the sex or age of patients with CH-B or CH-C (Table 1).

Treatment of Cultured Cells With Interferon-α. Huh-7 cells were treated with recombinant interferon-α (IFN-α) (Schering-Plough Corp., Osaka, Japan) at a concentration of 1000 IU/mL for 6 hours, and were harvested for analysis of induced gene expression by cDNA microarray.

Preparation of cDNA Microarray Slides. In addition to the in-house cDNA microarray slides consisting of 1080 cDNA clones as described,[13,15-19] we made a new cDNA microarray slide for a detailed analysis of the signaling pathways involved in metabolism and enzyme function in liver disease. Besides cDNA microarray analysis, a total of 256,550 tags were obtained from hepatic SAGE libraries (derived from normal liver, CH-C, CH-C related HCC, CH-B, and CH-B related HCC), including 52,149 unique tags. Among these, 16,916 tags with more than 2 hits were selected to avoid the effect of sequencing errors in the libraries. From these candidate genes, 9614 nonredundant clones were obtained from Incyte Genomics (Incyte Corp., Beverly, MA), Clontech (Nippon Becton Dickinson, Tokyo, Japan), and Invitrogen (Invitrogen Japan K.K., Tokyo, Japan). Each clone was sequence validated and PCR amplified by Dragon Genomics (Takara Bio, Otsu, Japan), and the cDNA microarray slides (Liver chip 10k) were constructed using SPBIO 2000 (Hitachi Software, Fukuoka, Japan) as previously described.[13,15-19]

Laser Capture Microdissection. Hepatocytes in liver lobules and infiltrated lymphoid cells in the portal area were isolated by LCM using a CRI-337 LCM system (Cell Robotics, Albuquerque, NM)[18] (Fig. 1). Frozen liver biopsy specimens in OCT compound were sliced into sections 8 μm thick, immediately fixed in methanol for 5 minutes, and kept on dry ice. Tissue samples were quickly stained with toluidine blue and dissected. Around 500 lymphoid cells and a similar number of hepatocytes were excised from 3 slides and immersed in a denaturing solution. Dissection was completed within 5 minutes for each slide.

RNA Isolation and Antisense RNA Amplification. Total RNA was isolated from liver biopsy samples using an RNA extraction kit (Micro RNA Extraction Kit, Stratagene, La Jolla, CA). Aliquots of total RNA (5 μg) were subjected to amplification with antisense RNA (aRNA) using a Message Amp aRNA kit (Ambion, Austin, TX) as recommended by the manufacturer. About 25 μg of aRNA was amplified from 5 μg of total RNA, assuming that 500-fold amplification of mRNA was obtained. Total RNA from LCM samples was isolated with a carrier nucleic acid (20 ng poly C) using RNAqueous-Micro (Ambion). The quality and degradation of the isolated RNA were estimated after electrophoresis using an Agilent 2001 bioanalyzer (Agilent Technologies, Palo Alto, CA) (Fig. 1B). RNA isolation typically yielded 20-40 ng total RNA from 500 cells. Half of the obtained RNA was amplified twice as described above to yield 20-40 μg aRNA. Antisense RNA (20 μg) was used for further labeling procedures. The optimum conditions of LCM and reproducibility of data were assessed repeatedly.

Hybridization on cDNA Microarray Slides and Image Analysis. As a reference for each microarray analysis, aRNA samples prepared from the normal liver tissue from 1 of the patients were used. Test RNA samples fluorescently labeled with cyanine 5 (Cy5) and reference RNA labeled with Cy3 were used for microarray hybridization as described.[13,15-19] Quantitative assessment of the signals on the slides was carried out by scanning on a ScanArray 5000 (General Scanning, Watertown, MA) followed by image analysis using GenePix Pro 4.1 (Axon Instruments, Union City, CA) as described.

Processing of cDNA Microarray Data. Hierarchical clustering of gene expression was performed by BRB-Ar-

Table 1. Characteristics of Patients, as Used for Analyses of Whole Liver Biopsy, LCM, and SAGE Samples

Patient No.	Virus	Age	Sex	ALT	A	F	Viral load (LEG/mL, KIU/mL)	HCV serotype	HBeAg	LCM Hep	LCM Ly
Whole liver biopsy samples											
1	HBV	34	F	45	1	1	8.2	na.	+		
2	HBV	64	F	119	1	1	>8.7	na.	+		
3	HBV	49	M	21	1	1	<3.7	na.	−		
4	HBV	29	M	194	2	1	7.5	na.	+		
5	HBV	47	M	10	1	2	<3.7	na.	−		
6	HBV	53	F	43	1	2	7.3	na.	+		
7	HBV	24	M	42	2	2	7.1	na.	+		
8	HBV	18	M	400	2	2	8.0	na.	+		
9	HBV	20	M	188	2	2	6.2	na.	+		
10	HBV	59	M	68	2	3	4.4	na.	+		
11	HBV	36	F	29	2	3	4.2	na.	−		
12	HBV	60	M	33	2	3	7.4	na.	+		
13	HBV	60	F	28	2	3	<3.7	na.	−		
14	HBV	35	F	145	3	3	7.6	na.	+		
15	HBV	64	M	48	1	4	7.1	na.	−		
16	HBV	55	M	30	1	4	7.4	na.	−		
17	HBV	34	F	45	2	4	8.5	na.	+		
18	HBV	54	M	159	2	4	5.5	na.	+		
19	HBV	60	M	121	3	4	4.6	na.	+		
20	HCV	24	M	34	1	1	>850	I	−		
21	HCV	68	F	43	1	1	720	II	−		
22	HCV	64	F	117	1	2	590	na.	−		
23	HCV	69	M	6	1	2	300	II	−		
24	HCV	42	M	59	1	2	410	II	−		
25	HCV	73	M	19	1	2	140	I	−		
26	HCV	43	M	98	2	2	60	I	−		
27	HCV	70	M	56	2	2	600	I	−		
28	HCV	70	F	26	2	3	350	I	−		
29	HCV	65	M	21	2	3	290	I	−		
30	HCV	47	M	225	2	3	120	I	−		
31	HCV	58	M	200	2	3	410	I	−		
32	HCV	57	F	116	2	3	490	I	−		
33	HCV	63	F	39	2	4	290	I	−		
34	HCV	76	M	54	2	4	660	I	−		
35	HCV	67	M	67	2	4	240	I	−		
36	HCV	46	M	111	2	4	>850	I	−		
37	HCV	63	M	64	2	4	60	na.	−		
LCM samples											
38(2)	HBV	64	F	119	1	1	>8.7	na.	+	+	+
39	HBV	31	F	114	1	1	8.5	na.	+	+	+
40	HBV	68	F	41	2	2	5.5	na.	+		+
41	HBV	29	M	140	2	2	>8.7	na.	+		+
42	HBV	40	M	80	2	2	<3.7	na.	−		+
43	HBV	45	M	83	2	3	6.1	na.	+		+
44(10)	HBV	59	M	68	2	3	4.4	na.	+	+	+
45(14)	HBV	35	F	145	3	3	7.6	na.	+	+	+
46(21)	HCV	68	F	43	1	1	720	II	−	+	+
47	HCV	47	M	33	1	1	50	I	−	+	+
48	HCV	67	M	80	2	2	114	II	−		+
49	HCV	73	M	71	2	2	>850	II	−		+
50	HCV	67	M	70	2	2	>851	I	−		+
51	HCV	59	F	43	2	3	>852	I	−		+
52(31)	HCV	58	M	200	2	3	410	I	−	+	+
53(32)	HCV	57	F	116	2	3	490	I	−	+	+
SAGE samples											
54	HBV	55	M	34	1	1	5.9	na.	−		
55	HBV	70	F	31	2	2	7.7	na.	−		
56	HBV	72	M	22	1	4	6.3	na.	+		
57	HCV	71	M	128	1	4	440	I	−		
58	HCV	69	F	84	2	4	212	I	−		
59	HCV	49	M	150	2	4	60	I	−		

Abbreviations: na., not applicable; LCM, laser capture microdissection; ALT, alanine aminotransferase; SAGE, serial analysis of gene expression; A, activity; Hep., hepatocyte obtained by LCM; Ly., lymphocyte obtained by LCM; F, fibrosis; No., if the sample was obtained from the same patient, the new sample number is shown with the old one; HCV RNA was assayed by Amplicor Monitor Test (KIU/mL); HBV DNA was assayed by transcription-mediated amplification (LEG/mL).

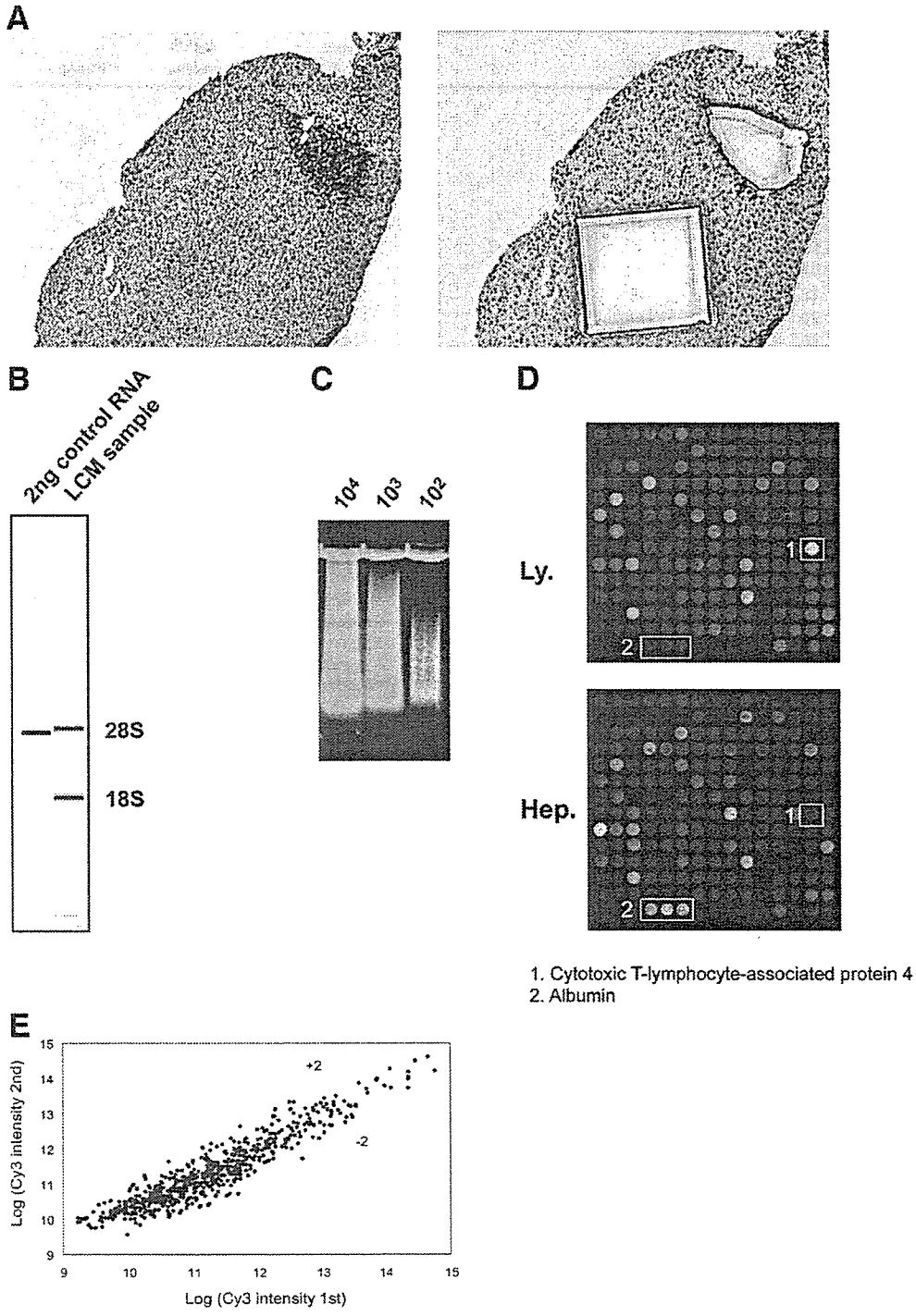

Fig. 1. Optimization of LCM and cDNA microarray analysis. (A) Toluidine blue staining of liver biopsy specimens before (left) and after (right) LCM. (B) Electrophoresis of isolated RNA using an Agilent 2001 bioanalyzer. (C) Two round-amplified aRNA from 10^2-10^4 excised hepatocytes. (D) Typical hybridization result from LCM samples. (E) Correlation of signal intensity between first and second amplified genes. Two values were significantly correlated ($P < .001$, $r^2 = .97$) within 2-fold differences.

rayTools (http://linus.nci.nih.gov/BRB-ArrayTools.htm). The filtered data were log-transferred, normalized, centered, and applied to the average linkage clustering with centered correlation. A class prediction was performed by compound covariate predictor incorporating genes that were differentially expressed at the $P = .002$ significance

Table 2. Supervised Learning Methods to Differentiate CHB and CHC

Classifier Category	Clinical Groups	Total Number of Cases	Number of Cases Misclassified	Classifier *P* Values	Number of Genes in the Classifiers ($P < .002$)
HBV versus HCV	HBV	19	1	<0.001	160
	HCV	18	3		
Histological stage	F1F2	17	10	0.402	55
	F3F4	20	7		
Histological activity	A0A1	13	6	0.173	106
	A2A3	24	6		
Age	≥50	22	9	0.298	39
	<50	15	6		
ALT at biopsy	≥80	14	7	0.200	21
	<80	23	6		

level as assessed by the random variance t test (BRB-ArrayTools). The univariate t test values for comparing the classes were used as the weights. The cross-validated misclassification rate was computed and at least 2,000 permutations were performed for a valid permutation P value. The Fisher and Kolmogorov-Smirnov tests were performed for gene ontology (GO) comparison ($P < .005$) (BRB-ArrayTools).

Pathway Analysis of Expression Data. The pathway analysis of the differentially expressed genes was performed using MetaCore software suite (GeneGo, St. Joseph, MI). Possible networks were created according to the list of the differentially expressed genes using the MetaCore database, a unique, curated database of human protein-protein and protein-DNA interactions; transcription factors; and signaling, metabolic, and bioactive molecules. The P value was calculated as:

$$p\text{-Value} = \frac{R!n!(N-R)!(N-n)!}{N!} \sum_{i=\max(r,R+n-N)}^{\min(n,R)} \frac{1}{i!(R-i)!(n-i)!(N-R-n+i)!}$$

where N is total number of nodes in the MetaCore database, R the number of network objects corresponding to the genes list, n the total number of nodes in each small network generated from the genes list, and r the number of nodes with data in each small network generated from the genes list. Moreover, direct interactions among the differentially expressed genes were examined. Each connection represents a direct, experimentally confirmed, physical interaction.

SAGE. Total RNA isolated from each of 3 patients with CH-B or CH-C was mixed to 200 μg in total, and polyadenylated RNA was extracted using a FastTrac mRNA Purification Kit (Invitrogen). The SAGE protocol was as described.[20,21] SAGE libraries were sequenced at random using an ABI Prism 377 DNA Sequencer and BigDye Terminator Cycle Sequencing Kit (PE Applied Biosystems, Foster City, CA). Sequenced files were analyzed with the SAGE version 1.00 software.

Quantitative Real-time Detection PCR. We performed quantitative real-time detection PCR (RTD-PCR) using TaqMan Universal Master Mix (PE Applied Biosystems). Primer pairs and probes for MxA, IP10, IFI15, OAS2, GZMA, TP53, PDECGF, IFNG, DIABLO, FGFB, BGA2, CASP9, PEX5, ANGPT1, VEGF, and β-actin were obtained from TaqMan assay reagents library. Results were expressed as means ± SEM. Significance was tested by 1-way ANOVA with Bonferroni's methods and differences were considered statistically significant at $P < .05$.

Results

Optimization of LCM and cDNA Microarray Analysis. Before analysis of region-specific gene expression, the sensitivity and reliability of linear aRNA amplification was examined. The quality and degradation of the isolated RNA were estimated after electrophoresis using an Agilent 2001 bioanalyzer (Fig. 1B). We successfully amplified aRNA from 10^2-10^4 excised hepatocytes with 2 rounds of amplification (Fig. 1C). The estimated amount of isolated RNA from around 150 excised hepatocytes (Fig. 1A) was 5-10 ng, and 10-20 μg of aRNA was obtained by 2 rounds of amplification, assuming that a 25×10^4-fold amplification (500-fold by single amplification) was carried out. A typical hybridization result is shown in Fig. 1D. Cytotoxic T lymphocyte-associated protein 4

Fig. 2. (A) Hierarchical clustering analysis of gene expression in hepatocytes and liver-infiltrating lymphocytes. Hep, hepatocyte; Ly, lymphocyte; B, hepatitis B; C, hepatitis C. (B) Hierarchical clustering analysis of 1,360 filtered genes (we excluded genes with an expression level within 1.5-fold of median value in more than 80% of samples) demonstrated more clear clusters of CH-B and CH-C.

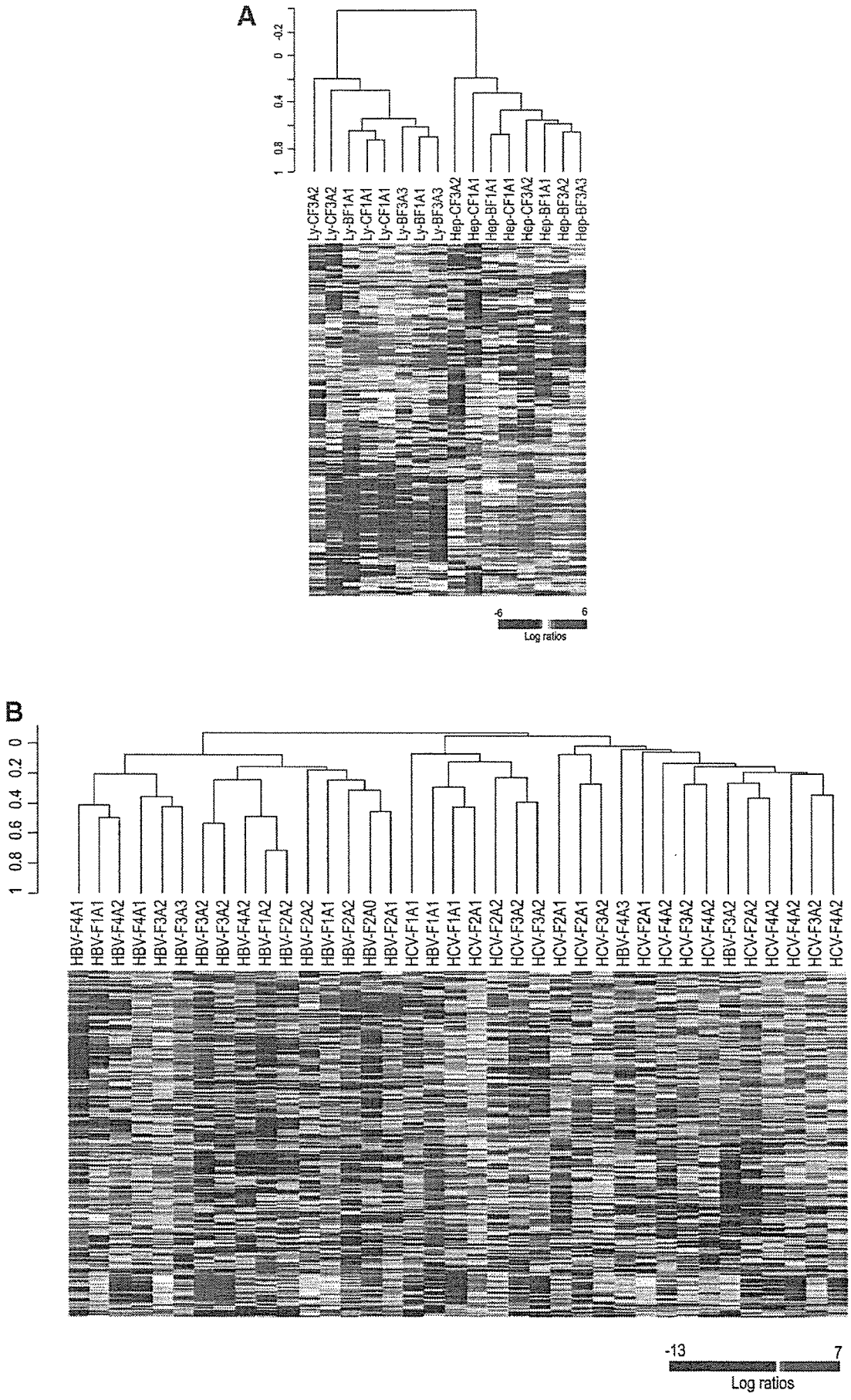
A
1 0.8 0.4 0 -0.2
Ly-CF3A2
Ly-CF3A2
Ly-BF1A1
Ly-CF1A1
Ly-CF1A1
Ly-BF3A3
Ly-BF1A1
Ly-BF3A3
Hep-CF3A2
Hep-CF1A1
Hep-BF1A1
Hep-CF1A1
Hep-CF3A2
Hep-BF1A1
Hep-BF3A2
Hep-BF3A3
-6
6
Log ratios
B
1 0.8 0.6 0.4 0.2 0
HBV-F4A1
HBV-F1A1
HBV-F4A2
HBV-F4A1
HBV-F3A2
HBV-F3A3
HBV-F3A2
HBV-F3A2
HBV-F4A2
HBV-F1A2
HBV-F2A2
HBV-F2A2
HBV-F1A1
HBV-F2A2
HBV-F2A0
HBV-F2A1
HCV-F1A1
HBV-F1A1
HCV-F1A1
HCV-F2A1
HCV-F2A2
HCV-F3A2
HCV-F3A2
HCV-F2A1
HCV-F2A1
HCV-F3A2
HBV-F4A3
HCV-F2A1
HCV-F4A2
HCV-F3A2
HCV-F4A2
HBV-F3A2
HCV-F2A2
HCV-F4A2
HCV-F4A2
HCV-F3A2
HCV-F4A2
-13
7
Log ratios

Fig. 2

was predominantly expressed in liver-infiltrating lymphocytes, whereas albumin was predominantly expressed in hepatocytes (Fig. 1D). To determine whether multiple amplifications affected the original gene expression, the signal intensities of first- and second-round amplified genes were compared. There was a significant correlation between the 2 values ($P < .001$, $r^2 = .97$), within a 2-fold difference (Fig. 1E), suggesting that the linear amplification procedure maintained the original level of gene expression.

Identification of Genes Differentially Expressed in Hepatocytes and Liver-Infiltrating Lymphocytes. Pairwise *t* test comparisons were applied and differentially expressed genes were identified in lymphocytes and hepatocytes in 4 patients with CH-B and 4 patients with CH-C (Supplementary Table 1-1). In hepatocytes, liver-specific proteins and enzymes such as fibrinogen, afamin, and cytochrome P450 were all expressed. In lymphocytes, cytokines, chemokines, and lymphocyte surface markers such as interleukin-7 receptor, chemokine (C-X-C motif) receptor 4, CD83 antigen, and CD69 antigen were all expressed (Supplementary Table 1-2). Hierarchical clustering analysis of gene expression in hepatocytes and liver-infiltrating lymphocytes demonstrated clear differences in gene expression (Fig. 2). Representative differentially expressed genes in lymphocytes and hepatocytes in CH-B and CH-C are summarized in Supplementary Tables 2-1, 2-2, 3-1, and 3-2.

Supervised and Nonsupervised Learning Methods to Classify Gene Expression Profiling According to Different Clinical Parameters. To examine which clinical parameters contributed to the changes in gene expression, supervised and nonsupervised learning methods were applied to classify gene expression profiles. The gene expression profiles of whole liver biopsy specimens, obtained from 19 patients with CH-B and 18 with CH-C, were analyzed. Hierarchical clustering analysis; a nonsupervised learning method, using 9641 nonfiltered genes, clearly demonstrated 2 clusters in CH-B and CH-C with a few exceptions (data not shown). Hierarchical clustering analysis with 1360 filtered genes (we excluded genes with an expression level within 1.5-fold of the median value in more than 80% of samples) demonstrated clearer clusters in CH-B and CH-C (Fig. 2B). Supervised learning methods based on the compound covariate predictor revealed that, among various clinical parameters including etiology (HBV or HCV), histological stage (F_1F_2 or F_3F_4), activity (A_0A_1 or A_2A_3), age ($\geq$50 or <50 years), and alanine aminotransferase (ALT) level at biopsy ($\geq$80 or <80 IU/mL), only etiology significantly classified these patients (Table 2). Thus, HBV or HCV infection determines gene expression to a greater degree than any other clinical parameters, such as histological stage and disease activity.

Differentially Expressed Genes in CH-B and CH-C Hepatic Lesions. The 160 genes were differentially expressed in CH-B and CH-C by class prediction analysis ($P < .005$); representative genes (greater than 3-fold difference in *t* value) are listed in Tables 3 and 4. Based on the expression profiles of hepatocytes and lymphocytes isolated using LCM, genes expressed in both hepatocytes and lymphocytes are described as Hep/Ly (Tables 3 and 4). Genes expressed at a significantly greater level in hepatocytes than lymphocytes were described as Hep. Genes expressed at a significantly greater level in lymphocytes than hepatocytes were described as Ly. In CH-B, genes involved in cell cycle arrest and induction of apoptosis were preferentially expressed. Several hepatocyte-specific and apoptosis-inducing genes such as Diablo homolog (cytochrome c/apaf-1/caspase-9 pathway activator) and BCL2-associated athanogene 2 (inhibitor of heat shock protein 70) were upregulated (Table 3, Fig. 7). In CH-C, cell cycle accelerating, immune-related, and antigen-presenting genes were preferentially upregulated. Many type 1 IFN-induced genes such as IFN-α-inducible protein 27 and IFN-α-inducible protein (clone IFI-15K) were upregulated in CH-C. The induction of these genes was confirmed by examining gene expression in Huh-7 cells treated with recombinant IFN-α (Tables 3 and 4, Fig. 7).

The frequent pathway processes observed in CH-B and CH-C using MetaCore are shown in Table 5. Induction of genes related to apoptosis (caspase activation via cytochrome C), transcription, and fibrosis (intermediate filament-based process and TGF-β receptor signaling pathway) were upregulated in CH-B, whereas genes related to immune reaction (defense response, antigen presentation, Golgi vesicle transport, and ubiquitin cycle), lipid metabolism (regulation of cholesterol absorption), and epidermal growth factor receptor (EGFR) signaling were upregulated in CH-C. This suggests that there are different signaling pathways in CH-B and CH-C.

Go Comparison of Expressed Genes in CH-B and CH-C Hepatic Lesions. The analysis of differentially expressed genes could underestimate the presence of mean full signaling pathways that were coordinately upregulated or downregulated, with subtle differences at an individual gene level. The biological significance of these coordinately regulated signaling pathways has recently been demonstrated.[22] Therefore, we applied the GO comparison tool to expressed genes in CH-B and CH-C hepatic lesions. The comparison tool provided a list of GO categories that were coordinately regulated between CH-B and CH-C.

Table 3. Differentially Upregulated Genes in Liver of Chronic Hepatitis B

Gene	GenBank ID	P Value	t Value HBV/HCV*	Hep/Ly	GO: Molecular Function
Viral genome					
HBV-core	X01587	0.000	6.69	Hep	Viral genome
Cell cycle and growth related					
V-ets erythroblastosis virus E26 oncogene homolog 2	NM_005239	0.001	3.97	Hep/Ly	skeletal development
RAP2A, member of RAS oncogene family	AI698376	0.000	3.91	Hep/Ly	signal transduction
Melanoma antigen, family C, 1	NM_005462	0.001	3.76	Hep/Ly	regulation of transcription
Cell division cycle 27	NM_001256	0.001	3.54	Hep/Ly	cell proliferation
Cyclin H	NM_001239	0.000	3.10	Hep/Ly	DNA repair
Immune response					
Interferon regulatory factor 6	NM_006147	0.000	3.80	Hep	regulation of transcription, DNA-dependent
Proteoglycan 2, bone marrow	R28336	0.001	3.65	Hep/Ly	defense response to bacteria
Chemokine (C-C motif) ligand 16	AW827147	0.001	3.49	Hep/Ly	chemokine activity
Janus kinase 2 (a protein tyrosine kinase)	NM_004972	0.001	3.48	Ly	JAK-STAT cascade
Chemokine (C-X-C motif) receptor 3	NM_001504	0.000	3.03	Hep/Ly	G-protein coupled receptor protein signaling pathway
Cell death					
BCL2-associated athanogene 2	NM_004282	0.000	3.95	Hep	apoptosis
Fas (TNFRSF6) associated factor 1	AA831837	0.001	3.74	Hep/Ly	apoptosis
Proline dehydrogenase (oxidase) 1	R88591	0.000	3.73	Hep/Ly	induction of apoptosis by oxidative stress
Caspase 9, apoptosis-related cysteine protease	NM_032996	0.001	3.58	Hep/Ly	apoptotic program
Purinergic receptor P2X, ligand-gated ion channel, 1	NM_002558	0.003	3.52	Hep/Ly	apoptosis
Tumor suppressing subtransferable candidate 1	NM_003310	0.002	3.35	Hep/Ly	apoptosis
Tumor necrosis factor (ligand) superfamily, member 11	NM_033012	0.002	3.25	Hep	cell differentiation
Diablo homolog (*Drosophila*)	NM_019887	0.004	3.04	Hep	apoptosis
Cell communication					
Nexilin (F actin binding protein)	NM_144573	0.000	4.15	Hep/Ly	unknown
Neurogranin (protein kinase C substrate, RC3)	NM_006176	0.000	4.09	Hep	signal transduction
Collagen, type XV, alpha 1	NM_001855	0.000	4.08	Hep/Ly	extracellular matrix
Chromogranin B (secretogranin 1)	NM_001819	0.001	3.47	Hep/Ly	hormone activity
Prostaglandin I2 (prostacyclin) receptor (IP)	NM_000960	0.001	3.42	Ly	G-protein signaling
Integral membrane protein 2C	NM_030926	0.002	3.36	Ly	integral to membrane
Sperm autoantigenic protein 17	NM_017425	0.002	3.26	Hep/Ly	cAMP-dependent protein kinase regulator activity
Talin 2	AF007154		3.18	Ly	cell adhesion
Cadherin 16, KSP-cadherin	AI241319	0.003	3.11	Hep	cell adhesion
Syntaxin binding protein 6 (amisyn)	AA281449	0.004	3.03	Ly	cell adhesion
Stress response					
RAD51-like 1 (*S. cerevisiae*)	NM_002877	0.000	3.78	Hep/Ly	DNA repair
Metallothionein 1X†	BC053882	0.001	3.44	Hep	electron transport
Siah-interacting protein	AA069322	0.002	3.08	Hep/Ly	ubiquitin cycle
Metallothionein 2A‡	NM_005953	0.004	3.03	Hep	copper ion homeostasis
F-box and leucine-rich repeat protein 2	NM_012157	0.000	3.01	Hep/Ly	ubiquitin cycle
Development					
Wolf-Hirschhorn syndrome candidate 1	NM_133335	0.001	4.51	Hep/Ly	morphogenesis
Homeo box B2	AI292043	0.001	3.87	Hep/Ly	development
Neurogenic differentiation 1	NM_002500	0.000	3.38	Hep/Ly	cell differentiation
Opiate receptor-like 1	NM_000913	0.004	3.29	Hep/Ly	G-protein coupled receptor protein signaling pathway
Wingless-type MMTV integration site family, member 2B	NM_024494	0.002	3.14	Hep/Ly	frizzled-2 signaling pathway
Cell motility					
Oligophrenin 1	R81942	0.001	3.80	Hep/Ly	rho GTPase activator activity
ATP-binding cassette, subfamily C, member 9	H16193	0.004	3.06	Hep	transporters
Transporter					
Sodium channel, voltage gated, type VIII, alpha	NM_014191	0.004	3.78	Hep/Ly	cation transport
Enzymes					
HMT1 hnRNP methyltransferase-like 6 (*S. cerevisiae*)	NM_018137	0.001	4.44	Hep/Ly	s-adenosylmethionine-dependent methyltransferase
Chymotrypsin-like	NM_001907	0.001	3.74	Hep/Ly	negative regulation of blood coagula
Aspartoacylase (aminocyclase) 3§	NM_080658	0.005	3.26	Hep/Ly	metabolism
Transcription and signal transduction					
Hepatocyte nuclear factor 4, gamma	AW273065	0.000	4.38	Hep/Ly	regulation of transcription
Nuclear receptor coactivator 6	NM_014071	0.000	3.98	Hep/Ly	DNA recombination
Protein kinase C, gamma	NM_002739	0.001	3.88	Hep/Ly	intracellular signaling cascade
T-box 2	NM_005994	0.000	3.82	Hep/Ly	development
Zinc finger protein 167	NM_018651	0.003	3.49	Hep/Ly	regulation of transcription, DNA-dependent
Small nuclear ribonucleoprotein polypeptide A	AI491862	0.002	3.37	Hep/Ly	intracellular signaling cascade
Zinc finger protein 266	NM_198058	0.002	3.03	Ly	regulation of transcription, DNA-dependent

*The univariate *t*-statistics for comparing the classes are used as the weights. †3.9-fold induction, ‡7.7-fold induction, and §1.8-fold induction by IFN-α in Huh-7 cells

In accordance with pathway analysis, antigen-presenting major histocompatibility complex molecules and IFN-α-induced genes were preferentially upregulated in CH-C (Table 6, Fig. 3). Genes related to apoptosis, DNA repair and cell death were upregulated in CH-B. DNA repair and apoptosis-related transcription factors were upregulated in CH-B, whereas anti-apoptosis and cell proliferation-related transcription factors were upregulated in CH-C. Platelet activating factor was upregulated in CH-C. As for metabolism-related gene regulation, peroxisome-associated genes were

Table 4. Differentially Upregulated Genes in Liver of Chronic Hepatitis C

Gene	GenBank ID	*P* Value	*t* Value HCV/HBV	Hep/Ly	IFN Induced	GO: biological process
Cell cycle and growth related						
Hect domain and RLD 5	NM_016323	0.000	4.50	Hep/Ly	7.7	regulation of cyclin dependent protein kinase activity
Inhibitor of growth family, member 4	NM_198287	0.001	3.50	Hep/Ly		grow arest
Phosphoinositide-3-kinase, class 3	AI446184	0.001	3.42	Hep/Ly		inositol or phosphatidylinositol kinase activity
Non-metastatic cells 1, protein (NM23A) expressed in	NM_000269	0.002	3.28	Hep		CTP biosynthesis
Mitogen-activated protein kinase kinase kinase 10	AI991621	0.003	3.23	Hep/Ly		JNK cascade
Immune responces						
Interferon, alpha-inducible protein 27	NM_005532	0.000	6.29	Hep	2.4	response to pest, pathogen or paras
Interferon, alpha-inducible protein (clone IFI-15K)	NM_005101	0.000	4.65	Hep/Ly	27.9	cell-cell signaling
Myxovirus (influenza virus) resistance 1	NM_002462	0.000	4.28	Hep/Ly	49.9	
Cold autoinflammatory syndrome 1	NM_183395	0.000	4.14	Ly		inflammatory response
Interferon-stimulated transcription factor 3, gamma 48kD	NM_006084	0.000	3.89	Hep/Ly	1.8	immune response
Beta-2-microglobulin	NM_004048	0.001	3.63	Hep/Ly	2.7	antigen presentation, endogenous antigen
2'-5'-oligoadenylate synthetase 2 (69-71 kD)	AA731148	0.001	3.49	Hep/Ly	3.3	immune response
Interferon-induced protein 44-like	NM_006820	0.001	3.42	Ly	4.5	immune response
Apolipoprotein L, 3	AW002766	0.003	3.23	Ly		inflammatory response
Immunoglobulin kappa constant	BC062732	0.004	3.04	Ly		immune response
Cell death						
Defender against cell death 1	NM_001344	0.000	4.11	Hep/Ly		apoptosis
HIV-1 Tat interactive protein 2, 30kDa	NM_006410	0.004	3.03	Hep/Ly		induction of apoptosis
Cell communication						
Major histocompatibility complex, class I, C	NM_002117	0.001	3.74	Hep/Ly		antigen presentation
CD97 antigen	NM_078481	0.001	3.72	Ly		cell adhesion
Major histocompatibility complex, class I, B	NM_005514	0.002	3.38	Hep/Ly	1.9	antigen presentation
Carcinoembryonic antigen-related cell adhesion molecule 5	NM_004363	0.002	3.30	Hep/Ly		integral to plasma membrane
Major histocompatibility complex, class II, DQ beta 1	NM_002123	0.002	3.25	Ly		antigen presentation
Major histocompatibility complex, class II, DR beta 4	NM_022555	0.002	3.25	Hep/Ly		antigen presentation
Dystroglycan 1 (dystrophin-associated glycoprotein 1)	AI684076	0.003	3.14	Hep/Ly		extracellular matrix
Dipeptidylpeptidase 6	NM_130797	0.004	3.11	Hep/Ly		integral to membrane
Ubiquitin and proteasome system						
Proteasome (prosome, macropain) subunit, beta type, 8	U17496	0.000	4.55	Hep/Ly		immune response
Ubiquitin D	NM_006398	0.003	3.13	Ly	2.1	antimicrobial humoral response
Proteasome (prosome, macropain) 26S subunit, non-ATPase, 2	NM_002808	0.004	3.05	Hep/Ly		regulation of cell cycle
Translation						
Eukaryotic translation elongation factor 1 beta 2	AI262506	0.000	4.46	Ly		protein biosynthesis
Eukaryotic translation initiation factor 1A, Y-linked	NM_004681	0.003	3.19	Hep/Ly	5.3	protein biosynthesis
Lipid metabolism						
Diacylglycerol O-acyltransferase homolog 1 (mouse)	NM_012079	0.002	3.31	Hep/Ly		O-acyltransferase activity
24-dehydrocholesterol reductase	NM_014762	0.003	3.19	Hep		cholesterol biosynthesis
Carnitine palmitoyltransferase II	NM_000098	0.005	3.01	Hep/Ly		fatty acid beta-oxidation
Nucleotide metabolism						
Adenosine deaminase, RNA-specific	NM_015841	0.001	3.46	Hep/Ly		RNA editing
Topoisomerase (DNA) I	J03250	0.003	3.22	Hep/Ly		DNA unwinding
THO complex 1	L36529	0.003	3.15	Hep/Ly		nuclear mRNA splicing, via spliceosome
Karyopherin alpha 3 (importin alpha 4)	NM_002267	0.003	3.14	Hep/Ly		NLS-bearing substrate-nucleus import
Nicotinamide nucleotide adenylyltransferase 1	NM_022787	0.004	3.06	Hep/Ly		NAD biosynthesis
Nuclear autoantigenic sperm protein (histone-binding)	M97856	0.005	3.00	Hep/Ly		DNA packaging
Ribonucleotide reductase M2 polypeptide	NM_001034	0.005	3.00	Ly		DNA replication
G protein binding protein						
Regulator of G-protein signalling 10	NM_002925	0.002	3.38	Hep/Ly		signal transduction
Transcription and signal transduction						
Staphylococcal nuclease domain containing 1	NM_014390	0.000	4.60	Hep/Ly		development
Ring-box 1	NM_014248	0.001	3.61	Ly		protein ubiquitination
Trophinin	NM_177558	0.001	3.44	Ly		embryo implantation
Forkhead box F1	AI453333	0.001	3.18	Hep/Ly	2.5	regulation of transcription, DNA-dependent
Nuclear antigen Sp100	M60618	0.003	3.02	Hep/Ly	5.8	regulation of transcription, DNA-dependent
Zinc finger protein 211	NM_198855	0.004	3.02	Ly		regulation of transcription, DNA-dependent
GA binding protein transcription factor, beta subunit 2, 47kDa	NM_181427	0.004	3.02	Hep/Ly		regulation of transcription, DNA-dependent
LIM protein (similar to rat protein kinase C-binding enigma)	AI445592	0.004	3.01	Hep/Ly		heart development
Hematopoietic cell-specific Lyn substrate 1	NM_005335	0.005	3.00	Ly		intracellular signaling cascade
ADP-ribosylation factor 5	M57567	0.005	3.00	Hep/Ly		intracellular protein transport

upregulated in CH-B, whereas cholesterol biosynthesis was upregulated in CH-C.

To investigate these findings in more detail, lymphocytes and hepatocytes were separately isolated by LCM and their gene expression was examined (Table 6, Fig. 4A, Fig. 7). Cyclophilin A and cyclophilin C, encoding peptidyl-prolyl cis-trans isomerases, were upregulated in CH-C. A recent report describes inhibition of HCV replication in Huh-7 cells by cyclophilin.[23,24] The upregulation of ssDNA-binding genes, such as p53 and RAD, and the relative downregulation of mitochondrial genes in hepatocytes, in CH-B, reflect a strong DNA damage response inducing apoptosis. Many IFN-α-induced genes were upregulated in hepatocytes rather than lymphocytes in CH-C.

CD4, CD8, linker for activation of T cells, and pro-apoptotic genes were upregulated in lymphocytes

Table 5. Pathway Analysis

Frequent Pathway Process	*P* Value
Whole liver tissue in CHB (n = 19)	
Caspase activation via cytochrome c	7.04E-11
Regulation of transcription, DNA-dependent	1.66E-12
Intermediate filament-based process	1.24E-07
Calcium ion transport	9.08E-08
Regulation of blood pressure	2.94E-07
Protein amino acid phosphorylation	4.04E-07
Regulation of angiogenesis	5.35E-09
TGF-beta receptor signaling pathway	8.08E-11
Whole liver tissue in CHC (n = 20)	
Defense response	3.27E-06
Antigen presentation, endogenous antigen	6.79E-06
Golgi vesicle transport	5.22E-07
Lipid catabolism	6.61E-06
Regulation of cell cycle	2.43E-08
Regulation of cholesterol absorption	1.02E-05
EGF receptor signaling pathway	1.59E-09
Ubiquitin cycle	4.71E-05

in CH-B. Despite the activated T cell responses in CH-B, chemokine expression was induced more in the lymphocytes in CH-C than lymphocytes in CH-B (Fig. 4A). To examine the functional role of liver-infiltrating lymphocytes further, LCM samples were also obtained from 4 more patients with CH-B and 4 with CH-C. Gene expression was compared for lymphocyte subsets (84 CD markers, including 26 T cell makers, 21 B cell markers, 16 myeloid cell markers, 11 NK cell markers, and 12 AD markers). Among these, many T cell markers and Th1 cytokines were significantly more upregulated in CH-B than in CH-C lymphocytes. Conversely, B cell marker, Th2 cytokines, and chemokines were preferentially induced in CH-C (Fig. 4B-C). The differences in immune reaction in CH-B and CH-C may be a reflection of their different pathogenesis.

Detailed Gene Network Analysis of Differentially Expressed Genes in CH-B and CH-C. To obtain a detailed and comprehensive gene network underlying CH-B and CH-C, SAGE data were integrated with those from cDNA microarray analysis. We applied 361 upregulated genes in CH-B ($P < .05$) and 344 in CH-C ($P < .05$), obtained from cDNA microarray analysis, and 1924 upregulated genes in CH-B (more than 5-fold tag count differences) and 1780 in CH-C, obtained from SAGE analysis, to the construction of the knowledge-based gene network. To find the gene network among these induced genes, published results of interaction of individual genes were integrated with these results using MetaCore software. Direct interactions between individual genes were searched for. The gene network of these differentially expressed genes formed a complex interaction of individual genes; however, representative signaling pathways underlying CH-B or CH-C were identified (Fig. 5).

In CH-B, p53 and 14-3-3 interacting genes might play an important role in the induced signaling pathways. Transcriptional factors such as CCAAT/enhancer binding protein (C/EBP), c-JUN, and cAMP-responsive element binding protein 1 (CREB1) are possibly also important molecules regulating these signaling pathways. These molecules induced apoptosis and activated transcription and oncogenes. Such activation might activate

Table 6. Gene Ontology Comparison

GO Description	Number of Genes	LS Permutation (*P* Value)	KS Permutation (*P* Value)	HBV	HCV	Reference
Whole liver tissue						
Antigen presenting	15	0.00105	0.034	1.01	1.49	0.81
IFN-alpha induced	71	$<1 \times 10^{-5}$	0.000	1.49	2.09	1.16
Cell death	34	0.005	0.019	1.35	1.15	0.99
DNA repair	62	0.005	0.041	1.51	1.10	1.11
G_1/S transition of mitotic cell cycle	18	0.001	0.009	1.25	1.41	1.23
Transcription factor binding	74	0.017	0.001	1.33	1.33	1.30
Cholesterol biosynthesis	12	0.029	0.002	1.11	1.44	1.30
PDGF	22	0.005	0.012	1.08	1.33	1.13
Peroxisome	19	0.026	0.005	1.46	1.17	0.93
Hepatocytes						
Peptidyl-prolyl cis-trans isomerase activity	9	0.002	0.001	1.31	1.48	1.15
Single-stranded DNA binding	16	0.019	0.003	1.85	1.34	1.27
Mitochondria	110	0.005	0.010	0.89	1.52	1.14
IFN-alpha induced	77	0.004	0.146	1.62	5.77	1.35
Lymphocytes						
Immunological synapse	12	0.002	0.003	6.38	3.78	3.31
Induction of apoptosis via deathdomain receptors	7	0.004	0.018	1.53	1.02	1.07
Chemotaxis	54	0.004	0.069	1.35	1.78	1.14

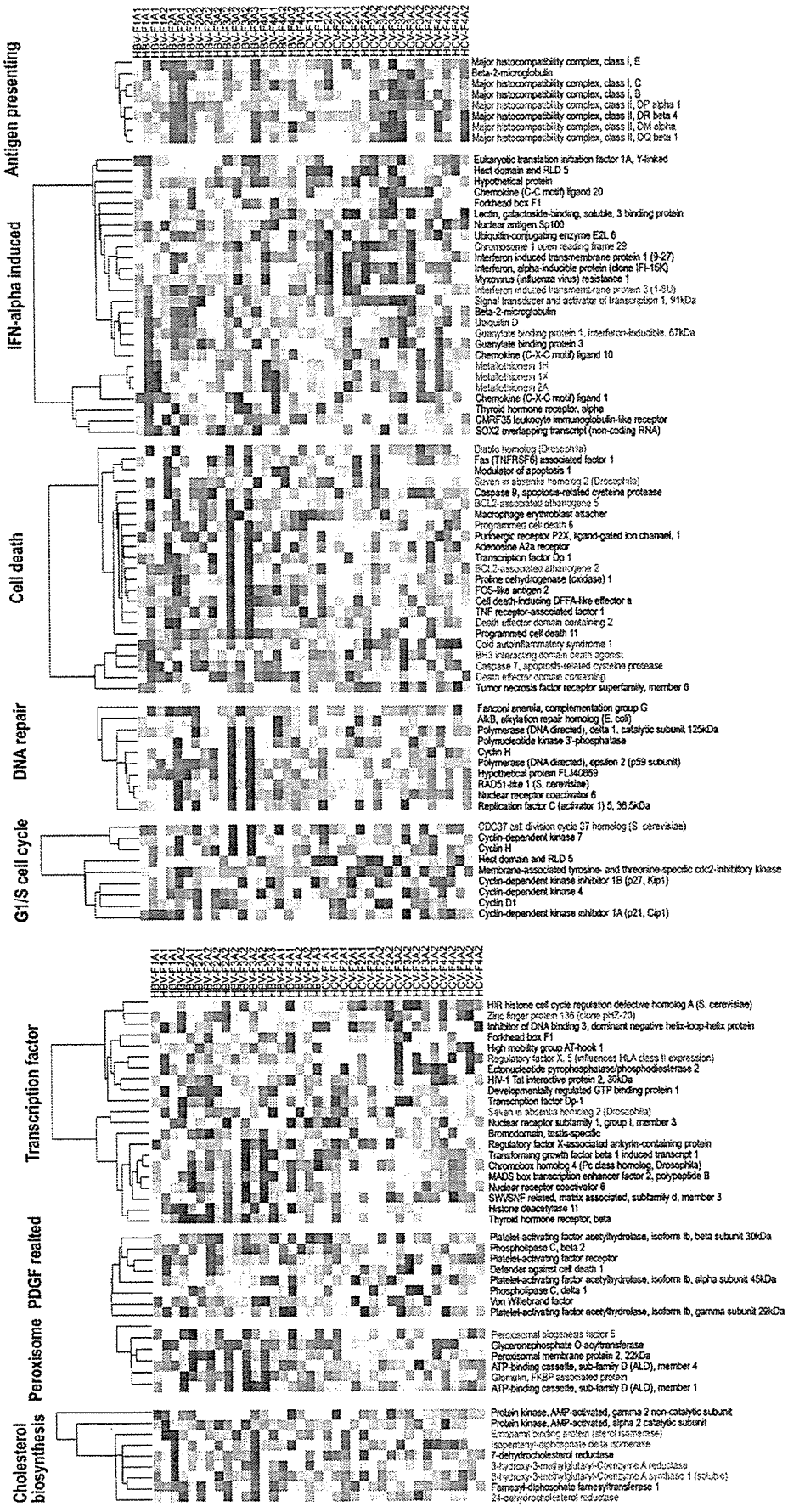

Fig. 3. One-way hierarchical clustering of whole liver samples with representative genes ($P < .05$) included in each GO category which was significantly different in CH-B and CH-C ($P < .005$). Green text denotes genes expressed predominantly in hepatocytes, and blue text denotes genes expressed predominantly in lymphocytes.

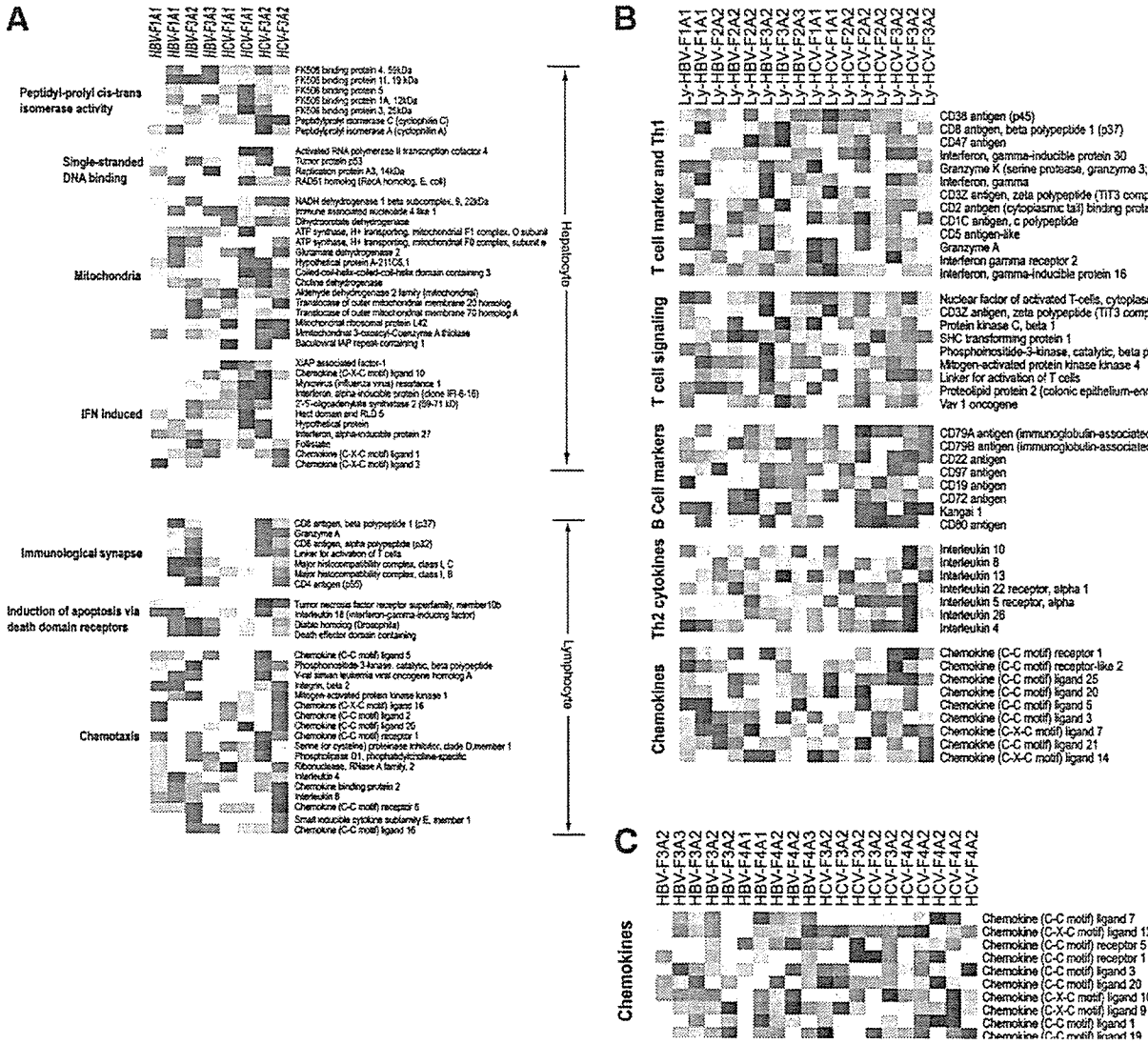

Fig. 4. (A) One-way hierarchical clustering of LCM samples with representative genes ($P < .05$). (B) One-way hierarchical clustering of liver-infiltrating lymphocytes, featuring specific gene sets of immune function. (c) One-way hierarchical clustering of whole liver sample gene sets of chemokines.

peroxisomes in CH-B (Fig. 5). In CH-C, type 1-IFN signaling (ISGF3/STAT1) might play a major role in the induced signaling pathways. The activation of the NF-κB and epidermal growth factor receptor (EGFR) signaling pathways may reflect liver inflammation and regeneration. These activations could lead to activation of liver X receptor/retinoid X receptor (LXR/RXR), a regulator of lipid metabolism.

Based on the database of MetaCore, which covers the entire regulation of the transcriptional factors, transcriptional regulation of differentially expressed genes was analyzed (Table 7). Transcription of mothers against decapentaplegic homolog 3 (SMAD 3), activator protein-1 (AP-1), p53, CREB1, and sterol regulatory element binding transcription factor 1 (SREB-1) was induced in CH-B, whereas NF-κB, IRF-1, STAT1, and retinoid acid receptor-alpha (RARα) signaling pathways were induced in CH-C. These differences fundamentally explain the different signaling pathways in CH-B and CH-C.

To examine whether these differences in gene expression contribute the different mechanism of hepatocarcinogenesis, we compared the angiogenic factors in CH-B and CH-C. The hierarchical clustering of patients using 34 angiogenesis-related genes obtained from cDNA microarray analysis, significantly clustered patients into 2 groups of CH-B or CH-C ($P = .0001$) (Fig. 6A). In CH-B, VEGF-family genes, FGF, and the angiopoietin